TAMPEREEN TEKNILLINEN YLIOPISTO
TAMPERE UNIVERSITY OF TECHNOLOGY

BAO-NGOC HUYNH

PROTEIN ADSORPTION ON BIOACTIVE GLASSES

Master of Science Thesis

Examiner: Associate Professor
Jonathan Massera
Examiner and topic approved on
09.08.2017

ABSTRACT

BAO-NGOC HUYNH: Protein adsorption on bioactive glasses
Tampere University of Technology
Master of Science Thesis, 56 pages, 02 Appendix pages
August 2018
Master's Degree Programme in Materials Science and Engineering
Major: Polymers and Biomaterials
Examiner: Associate Professor Jonathan Massera

Keywords: bioactive glasses, phosphate-based, protein adsorption, APTES, silanization

Protein adsorption is a critical biological event taking place whenever a foreign body is introduced to the human body, playing a key role in deciding subsequent cellular responses. It is also an important indicator of a material's biocompatibility. However, protein adsorption on bioactive glasses, which are a special class of biomaterials due to their peculiar biocompatibility and dissolution mechanisms, has not been fully understood.

The ability to immobilize two model proteins, i.e. bovine serum albumin (BSA) and fibronectin, of several bioactive glass compositions were assessed and improved by different surface treatments, namely washing in buffer solutions with varied pH values and functionalization with a silane coupling agent – (3-aminopropyl)triethoxysilane (APTES). The purposes of surface treatments were to improve the APTES grafting and glass surface charge for BSA and fibronectin grafting. The effects of surface treatments on wettability and surface chemistry were investigated using contact angle measurements and Fourier-transform infrared spectroscopy (FTIR), respectively. The presence of proteins on glass surface were evidenced by fluorescence imaging and were later correlated to fibroblasts adhesion.

Contact angle data show that the washing treatments slightly raised the wettability of bioactive glasses, thus modestly facilitating the adsorption of protein. A remarkable increase of the contact angle in APTES coated samples was the evidence of a successful silanization, which was expected to significantly enhance the protein adsorption via interaction between functional groups of proteins and APTES. Imaging of fluorescently-tagged proteins confirmed that APTES coated surface immobilized a greater amount of proteins and featured a more uniform protein layer. Subsequent cell culture tests showed that the improved protein adsorption by the surface treatments did support cell adhesion and spreading with larger cells and multiple focal adhesions detected. The results of this study propose a potential pathway to improve protein adsorption on both new and traditional bioactive glass compositions, which is promising toward the expansion their current application range.

ACKNOWLEGDEMENTS

This thesis work was conducted at the Institute of Biosciences and Medical Technology (BioMediTech). This is the result of the collaboration between Bioceramics, Bioglasses and Composites Group led by Associate Professor, Academy Research Fellow Jonathan Massera and Protein Dynamics Group led by Associate Professor Vesa Hytönen.

I would like to express my deepest gratitude to my supervisor Jonathan Massera for offering me a challenging project from which I have learned so much and for his smart guidance and advice. Thank you for your supports throughout the course of this challenge, the trust you put in me and your patience. My special thanks to Associate Professor Vesa Hytönen and his excellent research group for providing materials and immense assistance, and for the warm welcome you offered when I came to Arvo.

I wish to send my special thanks to Ayush Mishra as well as other colleagues from Bioceramics, Bioglasses and Biocomposites Group for their enjoyable instructions and company in the laboratory from the earliest days. I also wish to thank Rolle Rahikainen and Latifeh Azizi from Protein Dynamics Group for providing important help as I entered a new and challenging area. I truly appreciate your company, Lati, which I particularly enjoyed, during the long hours working with cells and the exciting cell imaging.

Finally, I wish to thank my family, my parents and my lovely friends for their love and support. Mother, I hope I have made you proud. And thanks Hoang, I would not be here if it were not because of you, my love and my strength.

Tampere, 20.08.2018

Bao-Ngoc Huynh

CONTENTS

LIST OF SYMBOLS AND ABBREVIATIONS

A.U.	Arbitrary Unit
ACP	Amorphous Calcium Phosphate
AFM	Atomic Force Microscopy
APTES	(3-aminopropyl)triethoxysilane
ATR	Attenuated total reflection
BCC	Body-centered cubic
BG	Bioactive glass
BO	Bridging oxygen
BSA	Bovine Serum Albumin
Ca	Calcium
CaO	Calcium oxide
DNA	Deoxyribonucleic acid
DSC	Differential scanning calorimetry
DTA	Differential thermal analysis
FCC	Face-centered cubic
FDA	Food and Drug Administration
Fn	Fibronectin
FTIR	Fourier-transform Infrared Spectroscopy
HCA	Carbonated Hydroxyl Apatite
HA	Hydroxyl Apatite
MEFs	Mouse Embryonic Fibroblasts
Na	Sodium
Na_2O	Sodium oxide
NBO	Non-bridging oxygen
P	Phosphorus
P_2O_5	Phosphorus pentoxide
PBS	Phosphate-buffered saline
PDMS	Polydimethylsiloxane
PFA	Paraformaldehyde
pI	Isoelectric point
PO_4	Phosphate group
PS	Polystyrene
RNA	Ribonucleic acid
SBF	Simulated body fluid
SEM	Scanning Electron Microscopy
SFG	Vibrational Sum Frequency Generation Analysis
Si	Silicon
SiO_2	Silica
TEM	Transmission Electron Microscopy
T_g	Glass transition temperature

1. INTRODUCTION

Foreign body reaction is a sequence of events taking place whenever a foreign material is introduced into the body, for example upon the implantation of a dental prosthesis. The first event that happens upon the implantation is the invasion of water and plasma proteins to the surface of the material and subsequently, immune cells such as monocytes, neutrophils and macrophages are recruited to the sites and adhere onto this protein-coated surface. The implant could interact well with our body and encourage wound healing or be isolated by a fibrous capsule or in the worst case, be considered as a harmful entity and provoke severe inflammation. The course of foreign body reaction heavily depends on the surface properties of the material which indicate its biocompatibility. (Anderson et al. 2008).

Biocompatibility of a material, i.e. the ability to exist in harmony with human body, is the main criteria to assess its safety for biomedical applications. Metallic materials have been utilized extensively in orthopedics or other medical implants for their high mechanical strength, long usage history, affordability. Polymers materials, although being younger in service in the biomedical fields, also claim their positions thanks to the versatility and tailorability as well as the controlled release mechanism of incorporated drugs. However, the biocompatibility standard of most medical grade metals and polymers is only to perform the intended functions without causing any harm to the body. (Anderson et al. 2008).

Ceramics, on the other hand, stands out among all biomaterial families for its natural biocompatibility because they can form stable bonds with proteins and living cells, in other words, being integrated to our body instead of being ignored like polymers and metals (Cao & Hench 1996). Certain types of bioceramics even exhibit the ability to promote a desired biological response such as bone regeneration (Cao & Hench 1996). Bioactive glass is a special class of bioceramics whose base components, e.g. SiO_2, Na_2O, CaO and P_2O_5, are friendly to physiological environment. When introduced to human body, these glasses gradually release their constituent ions, some of which eventually migrate back to the glass surface in the form of crystalline hydroxy carbonate apatite (HCA) (Cao & Hench 1996). HCA is similar to the naturally occurring mineral – hydroxy apatite – in our bones, thus recognized as a friendly entity and could interact with living cells, especially bone cells, or be degraded by osteoclasts (Cao & Hench 1996, Dee et al. 2003).

But how do the cells know that the surface that they encounter is friendly or hostile and how to behave? It all starts at the first few events taking place upon implantation – the

adsorption of water and proteins onto the surface of a material, which has a determining influence on subsequent events including cell adhesion and immune reactions. Cells do not actually see the surface of the material but only a thin layer of absorbed proteins. Therefore, the protein layer on the biomaterials surface could be considered as a communication channel between the materials and the living cells. If this protein layer consists of fully functional proteins whose orientation is favorable for cell adhesion, i.e. offering several cell binding sites, the subsequent reaction is more likely to be positive. Vice versa, if the proteins are denatured and lose their bioactivities, they might trigger negative immune reaction and eventually cause the failure of the implant. (Dee et al. 2003, Wang et al. 2012).

There have been many studies on bioactive glasses. Yet the level of understanding of this specific aspect, i.e. protein adhesion on bioactive glasses, is unsatisfactory. Given the peculiar nature and properties of bioactive glasses, e.g. continuous degradation, mineralized surface and the unusual nature of material-cell bonding, the properties of the protein monolayer deposited on their surface would be dynamic and feature unusual properties. Therefore, it is no exaggeration to say that this aspect, the bioactive glass surface – proteins interaction, deserves a greater attention, to allow controlling this process, thereby protein adsorption would be either enhanced or inhibited. Moreover, many studies directly correlate a material's biocompatibility to cell adhesion. Investigation on protein adsorption and influential factors on this aspect might be a better approach, cost and effort-wise, to deepen the understanding required not only to control cellular response but also to widen prospective application range for bioactive glasses.

In this study, we examined several bioactive glasses compositions, from commercial silica-based glasses to recently developed phosphate-based ones, and the properties, i.e. surface energy and electrical charge, surface composition and the evolution of surface chemistry during dissolution, which are proved to be important to protein adhesion. Surface treatments were conducted to improve the proteins (fibronectin and albumin) adsorption and the resultant effects was correlated to cell adhesions in cell culture tests. The results of this study would provide a better understanding of the glass surface – proteins interactions and pathways to improve the glass surface affinity to model proteins

2. THEORETICAL BACKGROUND

2.1 Bioactive glasses

2.1.1 Glass structure

To understand what bioactive glasses are, let us first familiarize ourselves with classical types of glasses and their structure. Glasses are often referred to as brittle and transparent class of inorganic materials that are used extensively in photonics, packaging, construction and decoration. The name comes from their "glassy" or amorphous structure as a solid and are traditionally made via conventional melting and quenching method where the ingredients are mixed in powder form, melted in furnace and cooled rapidly. They offer excellent chemical resistance and high optical transparency but are sensitive to crack propagation.

Soda-lime-silica glass is the most commonly used for windows and other light transmitting articles in construction. This is a silica-based composition with high content of silica, i.e. SiO_2, and other oxides such as CaO and Na_2O. Silicon's coordination number/number of valence electron is 4, thus being able to create 4 covalent bonds with 4 oxygen atoms, as shown in Figure 1. SiO_2 exhibits sp^3 hybridization and form a tetrahedron with 1 Si atom at the center bonding covalently with 4 oxygen atoms at the corners. Each oxygen in the corner is shared between 2 adjacent tetrahedral blocks and they play the role of connecting SiO_2 tetrahedral blocks together to build up a strong covalent network, thus called bridging oxygen. Therefore, SiO_2, as well as $-PO_4$ group in phosphate-based glasses and B_3O_6 in borate glass, are called network formers. (Bourhis 2014).

Other components of glasses are oxides of alkaline and alkaline-earth elements. They are called modifiers as they disrupt the glass network and reside in the interstitial spaces between these SiO_2 tetrahedrons. Modifiers give rise to the formation of non-bridging oxygen and ionic bonding instead of strong and stable covalent bond. For each oxygen to shift from bridging to non-bridging status, the SiO_2 tetrahedron it resides in loses a connection to a neighbor tetrahedron. That oxygen atom creates an ionic bond to the modifier atom using its spare electron as a compensation (Figure 2). The introduction of these modifier atoms weakens the SiO_2 network, thus also affecting the chemical resistance and lowering the glass formation temperature. Q_x is a terminology to classify the tetrahedrons' configuration in glass network based on their number of bridging oxygen x, reducing from maximum number of 4 to 0. The lower the number, the more isolated the tetrahedron is. (Bourhis 2014).

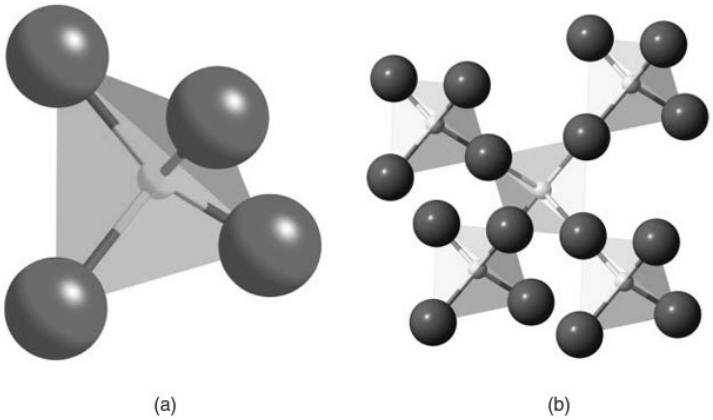

Figure 1. *Configuration of (a) a single SiO_2 tetrahedron and (b) a small network of 5 tetrahedrons. The dark spheres represent oxygen atoms while light ones represent silicon atoms. In the right picture, the middle tetrahedron possesses 4 bridging oxygen atoms, i.e. they perform the duty of connecting 2 adjacent tetrahedrons (Jones & Clare 2012).*

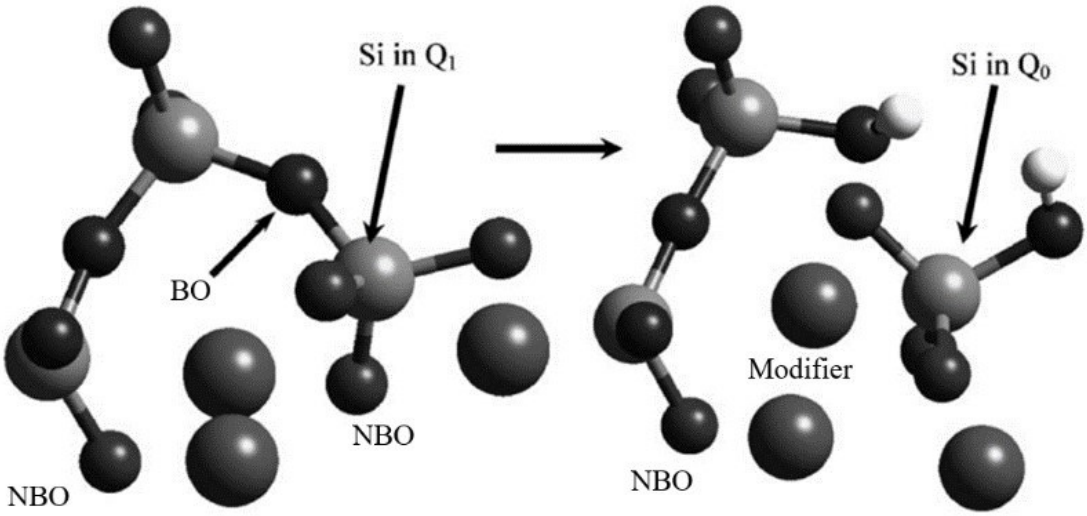

Figure 2. *Q_1 and Q_0 configuration. BO: bridging oxygen; NBO: non-bridging oxygen. Image adaptation from (Zeitler & Cormack 2006).*

These SiO_2 tetrahedrons can arrange themselves to create repeating units, like BCC or FCC units in metals, and ultimately a crystalline solid, e.g. quartz crystals, with long-range order during cooling from their molten state. Unfortunately, the required cooling rate to allow this re-arrangement is impractical. Instead, rapid cooling rate during quenching causes the viscosity of the molten/melt to increase gradually until it is too high for ion mobility, resulting in a frozen state of the random network of liquid. In this sense, solid glass features only short-range order and very much resembles the frozen structure of a liquid and is, therefore, often called a super-cooled liquid. Unlike a crystalline solid reaching its melting point where an abrupt change in physical properties, also known as a phase transformation, takes place, glasses experience a gradual transition over a temperature

span where the network becomes loose. Above this temperature span, glasses are viscous liquid while being an amorphous solid below it. From this temperature span, thermal analysis such as Differential Thermal Analysis (DTA) or Differentiate Scanning Calorimetry (DSC) is employed to determine glass transition temperature, T_g, which is important in determining the annealing temperature to release the thermal stress caused by volume contraction during glass formation process. (Bourhis 2014, Johnson & White 2013).

2.1.2 Bioactive glasses' reactions upon immersion

Bioactive glasses are a special type of glass, pioneered by Larry Hench in late 1960s in finding a solution for implant isolation, i.e. encapsulation of the implant by fibrous or scar tissue, when introduced into human body, which was the usual result when using metallic and synthetic polymer implants at that time (Cao & Hench 2006). Bioglass® 45S5 – the first bioactive glass – and other later developed bioactive glass systems have opened a new era of biomaterials and helped define again the term "biocompatibility", raising our hope of a new generation of biomaterials that can induce desirable responses and mend those defects in our body more effectively. These bioactive glasses generally exhibit an excellent biocompatibility in a way that not only they could exist harmoniously within the body without any negative immune-reactions but they also could create strong covalent bond to living cells and tissues and some can even promote bone regeneration. This difference between bioactive glasses and industrial glasses is that bioactive glasses usually contain high content of network modifiers, e.g. Na, Ca, as well as a small content of phosphorus. This combination allows moderate-to-fast dissolution and mineralization, i.e. the accumulation of Ca and P under the form of crystalline HCA, on the bioactive glasses' surface upon dissolution. (Jones & Clare 2012).

We will now take a closer look into the events occurring when bioactive glasses' surface is exposed to aqueous solution as well as the difference in dissolution mechanism between different glass systems. Hench explained the bioactivity of silica-based bioactive glasses using a 12-stage scheme where the 5 first stages describe the intrinsic surface reactions of glass network upon aqueous immersion (Cao & Hench 1996, Hench 2006). These 5 steps have been illustrated by Gunawidjaja et al. (2012) in their study and can be found in Figure 3.

Water invades the surface of bioactive glass and promotes rapid ion exchange between modifier ions such as Ca^{2+} and Na^{+} from the glass network and H^{+} or H_3O^{+} from the solution. This leads to the formation of silanol groups (Si-OH) in place of the lost modifiers ions and abandoned non-bridging oxygen atoms. This, together with the hydrolysis reaction of Si-O-Si or Si-O-P bonds, cause many SiO_2 tetrahedrons being converted to $Si(OH)_4$ and dissolving into the solution. Those silanol groups which do not go into the solution will polymerize, i.e. combine into siloxane bond Si-O-Si, and create a silica-rich layer, that thickens over time. The Ca^{2+} and PO_4^{2-} ions that leached out from the glass

network combining with those available in the body fluid and bloodstream create local supersaturation and reprecipitate to the glass surface. The silica-rich layer provides nucleation points for the newly formed mineral to attach onto the glass surface, creating an amorphous calcium phosphate ($CaO\text{-}P_2O_5$ – ACP) thin film. By continuously incorporating Ca^{2+}, PO_4^{2-} and other ions like CO_3^{2-} or F^- from the solution, a crystalline carbonated hydroxyl apatite (HCA) layer, whose composition is similar to hydroxyapatite (HA) – a mineral naturally found in bones, is built up over time. From this point on, many biological molecules and cells are offered a familiar and favorable surface to interact with. (Cao & Hench 1996).

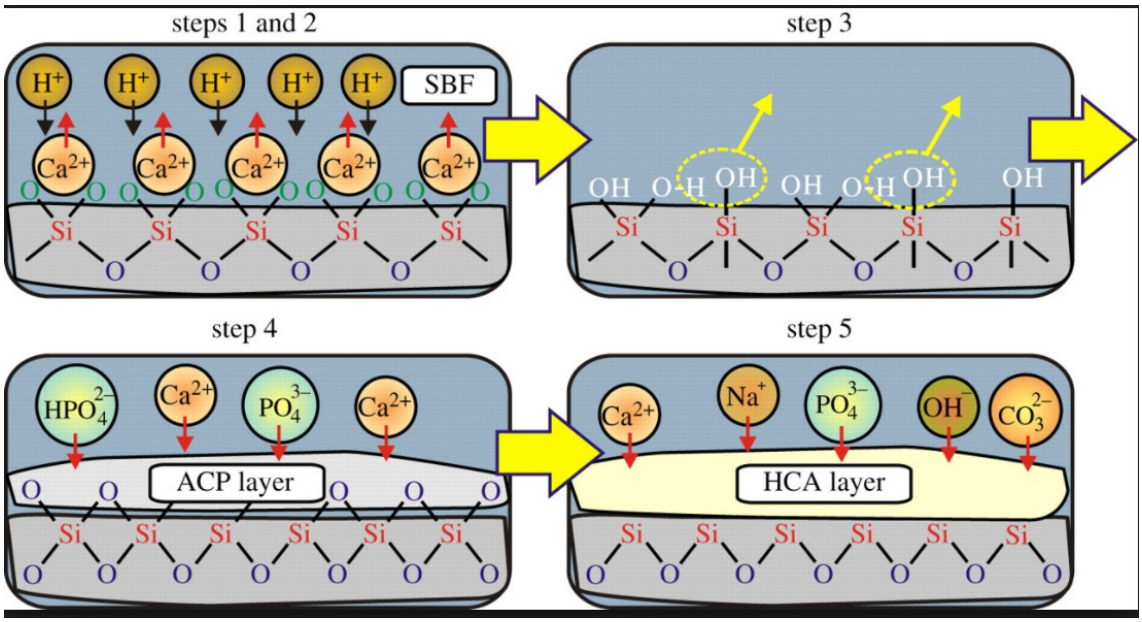

Figure 3. *The first 5 stages of bioactive glass reactions upon contacting aqueous environment, e.g. Phosphate buffered saline (PBS) or simulated body fluid (SBF). ACP: amorphous calcium phosphate; HCA: hydroxycarbonate apatite. (Gunawidjaja et al. 2012).*

2.1.3 Silicate-based and phosphate-based bioactive glasses

The previously described mechanism is called non-congruent dissolution and applied for silica-based bioactive glasses in a way that they always leave behind some insoluble silica gel as the result of the difference in leaching rate of different ions species. Due to the amorphous structure and tailorable compositions, several bioactive glass systems have been developed by adjusting the content of the constituent oxides within certain limits to achieve different dissolution rate and/or other beneficial effects depending on their intended applications (Hupa 2011). Bioactive glasses are classified based on the key network former species, e.g. SiO_2 in silica-based, PO_4^{3-} in phosphate-based and B_2O_3 in borate-based bioactive glasses (Figure 4). Among various bioactive glass compositions being investigated, 45S5, S53P4 and 13-93 are the most promising ones. They are already

approved by the Food and Drug Administration (FDA) or European regulatory authorities for biomedical applications.

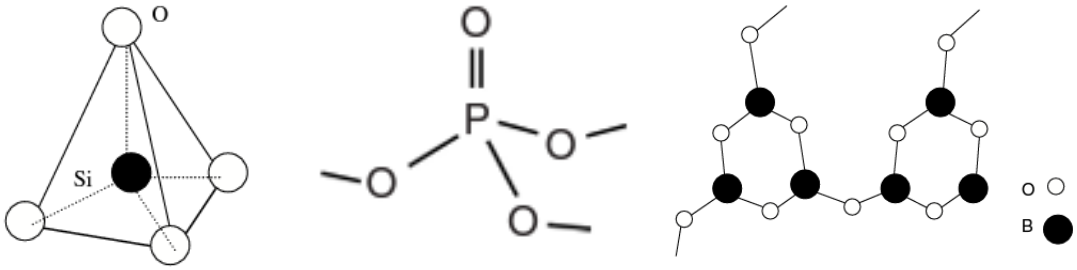

Figure 4. *Different network former species (Bourhis 2014 & Jones & Clare 2012).*

The original composition of the first bioactive glass 45S5 (Table 1) is usually considered as the starting point for other modified silica-based bioactive glass. S53P4 is one of many modified versions of 45S5 with 53 wt% of SiO_2 and 4 wt% of P_2O_5, also known commercially as BonAlive®, developed by Andersson et al., in 1990 in Finland as a substitute for bone graft. S53P4 features rapid dissolution and the unique property of strong inhibition of bacteria growth (Leppäranta et al. 2008, Lindfors et al. 2010b). 13-93 is another silica-based glass based on S53P4 formula, achieved by substituting part of Na_2O content with MgO and K_2O. 13-93 glass exhibits a much slower dissolution rate and enhanced processability (Fagerlund & Hupa 2017). In this study, we used S53P4 and 13-93 as references as their degradation are quite well understood and have shown promising results both in-vitro and in-vivo.

Table 1. *Compositions of 45S5, S53P4 and 13-93 glasses (adapted from Fagerlund & Hupa 2017).*

	45S5		**S53P4**		**13-93**	
Oxides	wt%	mol%	wt%	mol%	wt%	mol%
Na_2O	24.5	24.4	23	22.7	6	6
K_2O					12	7.9
MgO					5	7.7
CaO	24.5	26.9	20	21.8	20	22.1
P_2O_5	6	2.6	4	1.7	4	1.7
SiO_2	45	46.1	53	53.8	53	54.6

Non-congruent dissolution mechanism, i.e. non-uniform dissolution rate of constituent ions, is sometimes considered as a drawback of silica-based glass because they usually leave behind some remnants of insoluble silica gel in our body (Lindfors et al. 2010a). Phosphate-based bioactive glasses were recently developed to overcome many drawbacks of silica-based glasses, one of which is this incomplete dissolution mechanism. The dissolution mechanism of phosphate glasses is different to that of silica-based glasses. While the rapid ions exchange occurs in the beginning, as seen in silica-based glasses, chain

scission of phosphate network happens thereafter, leading to the release of full phosphate chains with similar composition to that of the initial glass. Phosphate-based bioactive glasses, therefore, allow complete dissolution and maintain their initial composition during the course of the dissolution. This feature is called congruent dissolution and considered one of the main advantages of phosphate glasses (Massera et al. 2016).

2.1.4 Surface modification methods

Although bioactive glasses are well-known for their excellent biocompatibility and ability to promote bone cell regeneration, their application range is limited by many drawbacks such as the unsatisfactory mechanical properties for bone grafting. Bioactive glasses are most commonly utilized under the forms of micro- or nanoscaled granules as bone cavity fillers, bioactive coatings for orthopaedic implants or scaffolds for bone tissue engineering (Ylänen 2011, p.107, p. 129, p. 189, p. 217). Since the discovery of angiogenesis property of bioactive glasses, many efforts have been made to investigate the prospects of using them for soft tissue constructions parallel to the previous focus on hard tissue engineering (Rahaman et al. 2011). This has led to a greater urge to deepen the understanding of the interactions between bioactive glass and physiological elements and ultimately to control them for a wider range of applications. Since bioactive glasses are inorganic materials and it takes time for the calcium phosphate layer to develop, surface chemistry modification, the introduction of different functional groups that are compatible to biomolecules, are the most common and effective methods to promote bioactivity of bioactive glasses (Dee et al. 2003, Ferarris & Verné 2017, McKenzie & Webster 2009).

Grafting bioactive glasses with 3-aminopropyltriethoxysilane (APTES) – a non-toxic coupling agent – is one option for surface chemistry modification and improving their compatibility with organic biomolecules thanks to the introduction of amine group -NH_2. Attempts have been made not only to improve the biocompatibility of bioactive glasses and improve their protein adhesion in general but also to incorporate other functional or therapeutic biomolecules such as alkaline phosphatase, bone morphogenic proteins and ibuprofen in drug delivery application (Ferraris & Verné 2017).

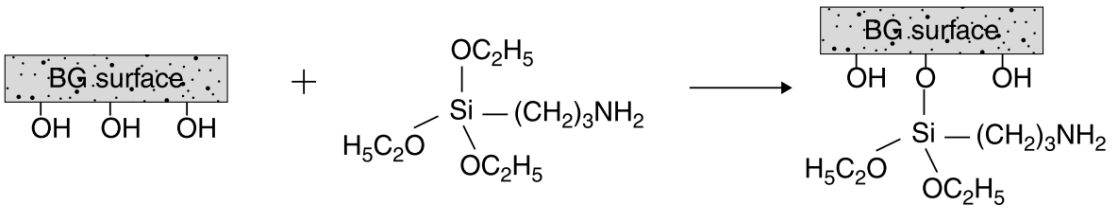

Figure 5. *Silanization reactions with APTES (BG: bioactive glass) (Chang et al. 2011).*

The APTES grafting reaction, also called silanization, requires the activation of both bioactive glass surface and APTES. Therefore, there is usually a washing step of bioactive

glass in aqueous solution to activate and increase the silanol (Si–OH) groups density on the surface prior to the grafting reaction, which usually later takes place in either aqueous, toluene or ethanol environment (Ferraris & Verné 2017). Functionalization, with APTES, of phosphate bioactive glass was later studied (Massera et al. 2016). It was found, even upon surface modification optimization, the level of APTES grafting was lower than in typical silica-based glasses, most likely due to the lower content of –OH group present at the surface of these glasses. This is attributed to the congruent dissolution of phosphate bioactive glasses (Massera et al. 2016).

2.2 Proteins

While Hench has described the mechanism of bioactive glass reaction upon introduction to the body, let us examine the other side, in other words, how those components from our body see and respond to the intrusion of a foreign body and what is the particular role of proteins in these processes.

2.2.1 Foreign Body Reaction

Whenever our body senses the sudden appearance of a foreign body such as bacteria or a splinter, it immediately sets up different defence acts to respond to this subject. Inflammatory reactions and wound healing process are well-known for their roles as our lines of defence against these harmful entities, although they might also be a problematic issue for the implantation of biomedical devices. They are, however, the consequences of a series of events taking place at the very moment when that foreign entity is introduced into physiological environment. This series of event, called foreign body reaction, has a pivotal role in deciding the fate of that foreign entity, thus being the topic for discussion in several literatures (Dee et al. 2003, Anderson et al. 2008, McKenzie & Webster 2009).

Almost immediately upon implantation, the surface of the foreign body is covered with water, thus possibly being affected or activated by this hydration. The next molecules to come to the surface, within a few milliseconds, are plasma proteins (proteins present in blood), e.g. albumin, fibronectin, vitronectin, fibrinogen or collagen, and it takes a few minutes to an hour to form a stable self-assembled protein layer. Together, they create a heterogeneous layer of proteins whose arrangement changes depending on the biomaterial surface and will affect to the following steps such as the anchorage of immune and repairing cells, e.g. neutrophils, macrophages or osteocytes (Dee et al. 2003, Anderson et al. 2008, McKenzie & Webster 2009).

A protein layer which is favorably arranged and oriented might expose many specific cell-binding sites, thus assisting the recognition and adhesion of certain cell types favorable for implant integration and tissue repair. If the protein molecules are adversely ordered and do not allow selective cell adhesion, the surface might soon be invaded by

macrophages and isolated by foreign body giant cells or in the worst case, trigger an acute or chronic inflammation (Anderson et al. 2008, McKenzie & Webster 2009).

This explanation is in fact a simplification. There are several factors, coming from both the proteins, the surface they interact with as well as the environment, that affect the characteristics of this layer and later on cell adhesion. The following parts are dedicated to give an overview on the protein structures and behaviours and other factors that can be altered to positively influence the protein adsorption.

2.2.2 Protein structures

Proteins interact differently with different substances and thus, it is important to understand the structure and bioactivities of proteins to realize the differences that we can make to improve this aspect.

Simply put, proteins are large chains of amino acids arranged in a predetermined manner by our genes. Each type of proteins thus exhibits different structure and functions, which enable them to participate in many processes such as foreign body recognition, extracellular matrix construction and biological process modulation. When considering a protein structure, a scheme of 4 levels of arrangement is usually used to describe it, namely primary, secondary, tertiary and quaternary structures (Dee et al. 2003, McKenzie & Webster 2009).

Primary structure of a protein is the combination and linear order of amino acids from a pool of 21 common amino acids in human body. The configuration of a general amino acid is shown in figure 6, consisting of an amino and carboxyl group with a side chain R. The side chain R could be non-polar or polar, positively or negatively charged and is the main difference between amino acids. These amino acids combine in a predetermined sequence to create a chain whose total charge and polarity could be affected by the pH of the environment. (Dee et al. 2003, McKenzie & Webster 2009).

Due to their great length and possible interactions mainly between amino and carboxyl groups, sometimes also the side chains, amino acid chains do not exist as straight band but possess a certain conformation such as α-helix (chain coiling) or β-sheet (chain folding in a parallel manner to make a band-like structure). These conformations are called secondary structure, indicating the 3D structure of short sections of the chain caused by the interactions between amino acids within close distance. (Dee et al. 2003, McKenzie & Webster 2009).

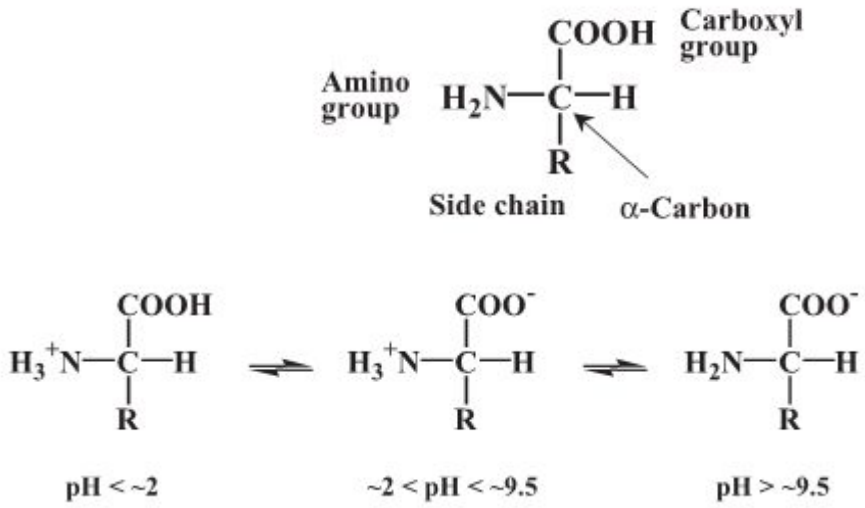

Figure 6. *Top: The configuration of amino acids.*
Bottom: The effects of pH on charge of amino acids (Dee et al. 2003).

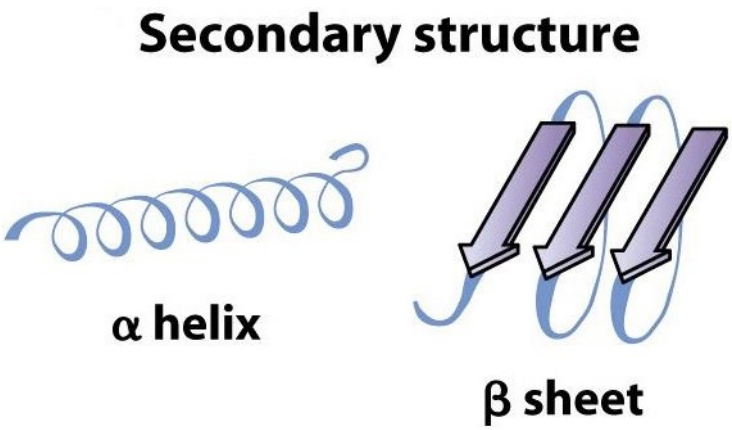

Figure 7. *Secondary structure of proteins: α-helix (chain coiling) and β-sheet (chain folding in a parallel manner to make a band-like structure)*
(McKenzie & Webster 2009).

Next level of structural arrangement is tertiary structure, involving the interactions of distant domains and the way they organize to create a 3D structure of a protein's subunit. In this level, the interactions between side chains, including covalent disulfide bonds, ionic bonds, hydrogen bonds and polar interaction, play the main role. The protein tertiary structure's main driving force is to assemble themselves in a way to minimize their repulsion force in body fluid by concealing hydrophobic and non-polar groups inside and exposing polar and hydrophilic groups. (Dee et al. 2003, McKenzie & Webster 2009).

The last level of arrangement is quaternary structure where multiple subunits combine to create a protein, typically via disulfide bonding. Proteins' quaternary structure, thus, indicates the number and the arrangement of the subunits they possess, e.g. dimer, trimer and tetramer for proteins consisting of 2, 3 and 4 subunits, respectively. Many theories

have been dedicated to explaining the driving force behind quaternary structure of proteins. One of them suggests that this quaternary arrangement is meant to simplify the process of protein production and minimize the risks of errors when uncoding RNA/DNA by assembling many short sequences or subunits. Hemoglobin is one example for a tetramer – it consists of 2 α chains and 2 β chains – while fibronectin is a dimer consisting of 2 subunits. (Dee et al. 2003, McKenzie & Webster 2009).

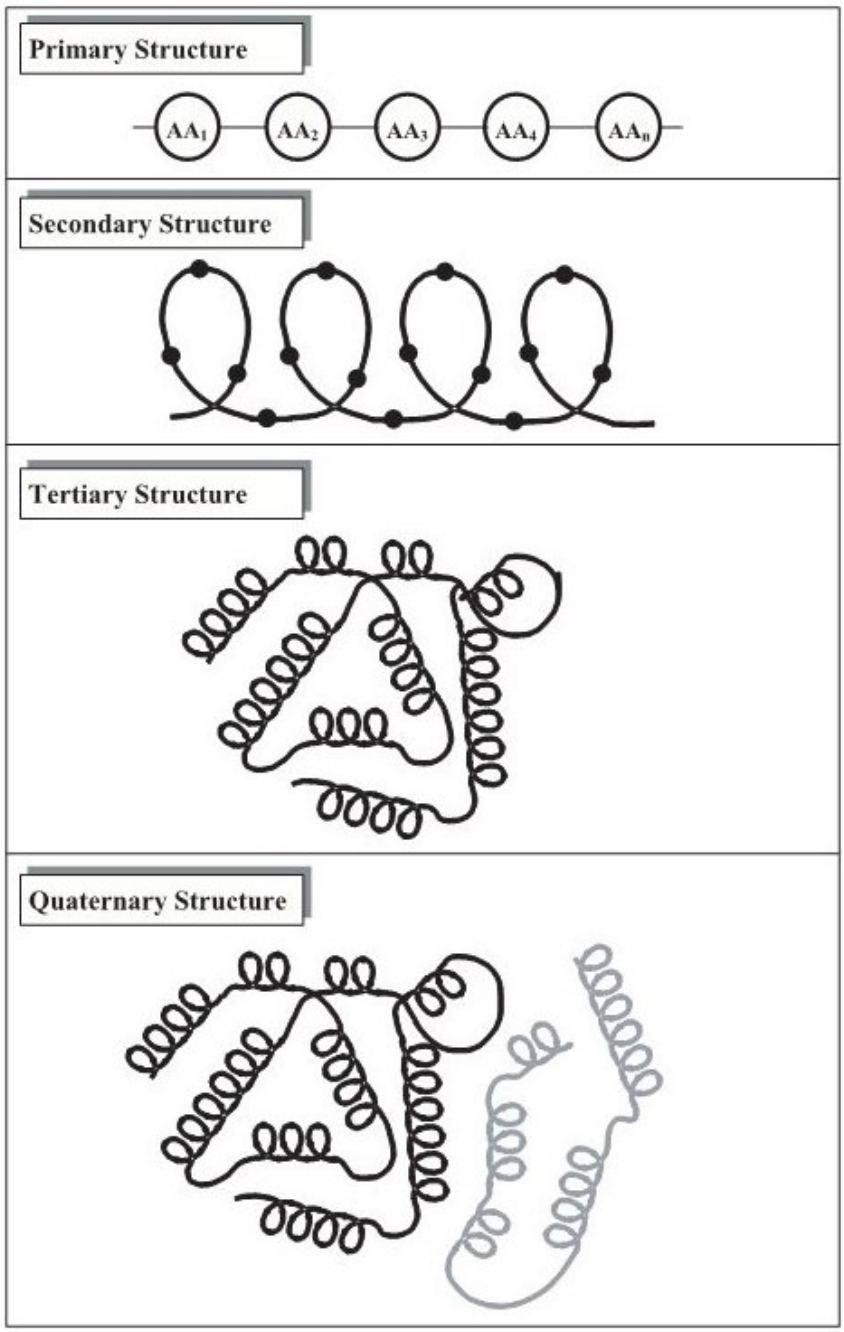

Figure 8. *Four levels of arrangement of protein structure (Dee et al. 2003).*

In brief, primary structure of a protein shows their genetic code as amino acid sequences and their adaptation mechanism to the environment pH and charge while the secondary structure gives the information of the original small domains' configuration. Secondary,

tertiary and quaternary structure might be used to examine conformational changes upon protein immobilization on a biomaterial surface, e.g. whether they maintain their original shape or spread and unfold. (Dee et al. 2003, McKenzie & Webster 2009).

2.3 Protein adsorption

Protein adsorption is an interesting matter not only because it has a determining effect on the subsequent cell adhesion and ultimately the fate of the foreign body but also due to the conformational changes protein experience upon adsorption. It demands a certain level of understanding to enable the ability to tailor our surface and the environmental conditions to optimize this aspect for prospective applications. For there are several influential factors coming from both the surface, the adsorbed proteins and the grafting conditions, we shall go through each group of these factors and their manifestation in our study (Dee et al. 2003, McKenzie & Webster 2009).

2.3.1 Surface properties

Since the interfacial region is where all the interactions and component exchanges take place, it is widely accepted that a material's biocompatibility largely relies on its surface properties. They are divided into different groups, namely geometrical, electrical and chemical properties.

Topographical features are physical patterns of a material surface such as pores, grains and grooves and the size and depth of them, giving the information of the general roughness and total surface area. One material which appears to be smooth to the eyes can be extremely rough and inhomogeneous at microscopic scale, particularly for proteins as they are of nanoscale. Atomic Force Microscopy (AFM), Scanning Electron Microscopy (SEM) or Transmission Electron Microscopy (TEM) are some of the microscopical methods often used to investigate the topographical features of a material (Scheibe et al. 1995). In general, a surface featuring a diversity of patterns such as grooves or pores offers a greater total area for proteins to explore and adhere on compared to a smooth one, even though they are of the same material. Moreover, the dimensions of these patterns are also of great importance since materials with nano-roughness are proved to have a more remarkable affinity to proteins compared to ones with microscaled roughness (Dee et al. 2003, McKenzie & Webster 2009).

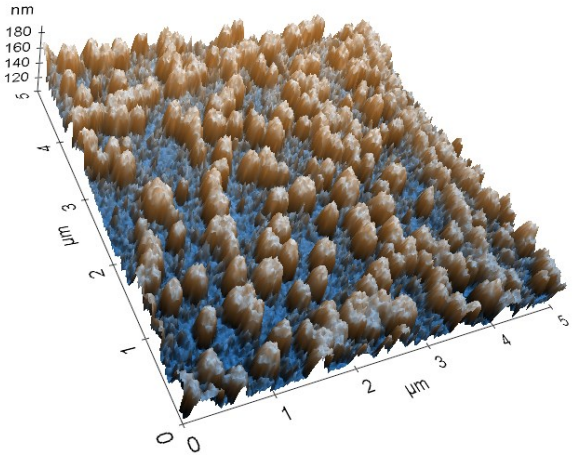

Figure 9. *Topography of a S53P4 (silica-based) glass disk washed with acidic buffer solution, collected using AFM method.*

Before the proteins come probing the surface, water molecules are the first to invade and explore the surface and later give a guidance for proteins on how to interact with it. Surface energy, surface potential and chemistry are the 3 features that relate closely to each other and give hints on how a surface interacts with water and proteins.

Surface energy is another important property affecting protein interactions as it indicates how easy a solution can wet its surface. In the case of protein solutions, the liquid of interest is water, containing also other components such as electrolytes. Surface energy allows us to predict the prospect of the protein immobilizing capacity of a material by revealing its wettability when coming in contact with protein solutions, in other words, its hydrophilicity or hydrophobicity. A common analysis method used to determine surface energy is contact angle measurement. A hydrophobic surface exhibiting contact angle value greater than 90 degrees could generally immobilize more proteins and create a more tenacious binding (Dee et al. 2003). However, Kim et al. suggest that the orientation of proteins on hydrophobic surface might not be as highly ordered as in hydrophilic surfaces (Kim & Somorjai 2003).

Because the aqueous environments also contain electrolytes, there can be interactions between the electrolytes and the surface via electrostatic forces. The inhomogeneity of a surface can cause a non-uniform distribution of these electrolytes and water, thus resulting in different orientations of water molecules and proteins. A property that is highly related to a material's surface energy is surface charge or surface potential. This property shows its tendency to attract counter-ions from the solution to the interface when coming into contact with a liquid. This value can be measured using streaming potential method and very useful to predict the prospect of protein adhesion (McKenzie & Webster 2009).

Although it used to be doubtful that cells can distinguish between materials of different chemical compositions, many research works show that proteins may exhibit affinity towards a certain type of surface that features a compatible surface chemistry thanks to the variety of amino acids' side chain R chemical structure as explained in protein primary structure. Surface chemistry dictates the protein species adsorbed on the surface, possible bond types and strength as well as possible reactions. While an enhanced surface potential and wettability could only support physical attractions between proteins and the surface, the introduction of functional groups on the surface could lead to a stable chemical bondand positively affect the orientation of the protein layer (Chang et al. 2011, Ferraris & Verné 2017).

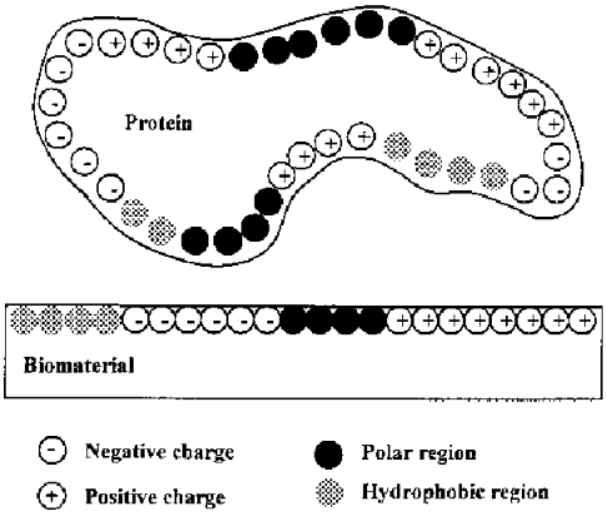

Figure 10. *Possible surface-protein interactions through electrostatic force or polarity compatibility. (Dee et al. 2003)*

2.3.2 Proteins and the environment

We shall continue with the other parties in the event which are proteins and the medium where the adsorption takes place. As mentioned in the previous part, proteins exhibit highly interactive structures with many functional groups varying in size, charge and hydrophilicity. Their structures, therefore, could "improvise" to interact with different substances or environments. When suspended in aqueous environments such as the body fluid, proteins generally conceal hydrophobic and non-polar domains inside while expose hydrophilic and polar groups. However, protein total charge could be altered by the pH and ionic concentration of the solution and can reach a neutral value at their isoelectric point (pI), i.e. the pH value where the total charge of the protein chain in solution is zero. The repulsive force between protein molecules at this point is minimized, which allows them to adsorb more readily onto a surface (Dee et al. 2003, McKenzie & Webster 2009).

Each protein species has their own isoelectric point, for example, Bovine Serum Albumin (BSA) has a pI value of 4.7 while fibronectin's pI value is from 5.5 to 6. The understanding of the isoelectric point is, thus, especially useful for applications where only a specific type of proteins needs to be grafted onto the surface and should be deployed to optimize the pH value and the ionic strength of this single-component solution (Dee et al. 2003).

While one can prepare a single-component protein solution to optimize the adsorption process when required, physiological environment and other simulated fluids such as cell culture medium are multi-component solutions. It is therefore more relevant to consider the competitive adsorption between different protein species, their density and conformations of the protein layer as these characteristics are considered the guideposts for possible outcomes of the contact (Dee et al. 2003, McKenzie & Webster 2009).

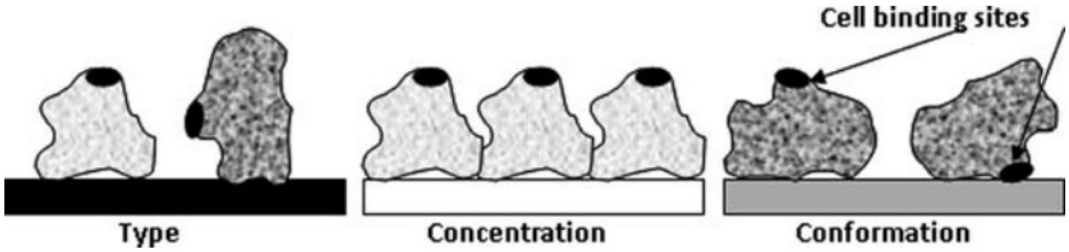

Figure 11. *Protein layer variables that can affect the subsequent cellular responses (McKenzie & Webster 2009).*

In a multi-component medium such as human blood where more than 150 proteins wander and could deposit on a surface, the hierarchy of protein deposition and the types of proteins found in the protein layer largely depend on their affinity and availability. A few types of protein can arrive early at the surface due to their small size, great diffusion coefficient and high concentration in the solution, in other words, high availability. However, they can detach and be replaced by other protein species that have greater affinity for the surface, determined by their preferential compatibility in electrical charge and orientation of functional groups. The protein adsorption and desorption proceed until the protein layer reach a stable state where all the proteins have a strong and irreversible interaction to the surface. Fibrinogen has higher affinity than albumin, thus usually causing the desorption of albumin and dominating the surface despite its much slower rate of arrival (Dee et al. 2003).

After a stable and irreversible protein layer is established, cells arrive and interact with this layer via two mechanisms: non-specific and specific interactions. In the former interacting mechanism, only physical interactions such as electrostatic forces or van der Waals force are involved while cells can bind to protein molecules via receptor-ligand bonds in later mechanism. Arginine-Glycine-Aspartate (Arg-Gly-Asp or RGD) – the minimal cell-recognizable sequence – and heparin binding domains are some examples of such ligands in specific cell-protein interactions. Proteins featuring more specific cell binding sites

such as fibronectin, vitronectin, fibrinogen, laminin and collagen play important role in supporting subsequent cell adhesion. Bovine serum albumin (BSA), on the other hand, does not contain this RGD sites or any other specific ligands, thus attending non-specific cell adhesion only. (Dee et al. 2003, Lamba et al. 1998, McKenzie & Webster 2009).

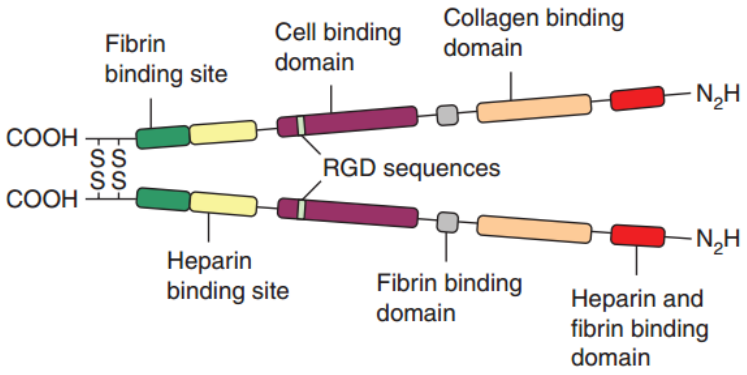

Figure 12. *Structure of fibronectin with several binding domains (Badylak 2008).*

Moreover, protein adsorption is not a static but a dynamic process where the adsorbed proteins feature time-dependent spreading and unfolding. The spreading and unfolding rate depends not only on the hospitality of the surface but also on the structural stability of the protein itself. A protein is considered as soft if it possesses fewer cross-linking and is prone to conformational changes and ultimately, denaturation. A hard protein, on the other hand, would be able to retain some extent of their structure and biological functions such as catalyzing and mediating cell adhesion. During these spreading and unfolding, proteins have the options to reveal more specific cell binding sites or to conceal them. (Dee et al. 2003, McKenzie & Webster 2009).

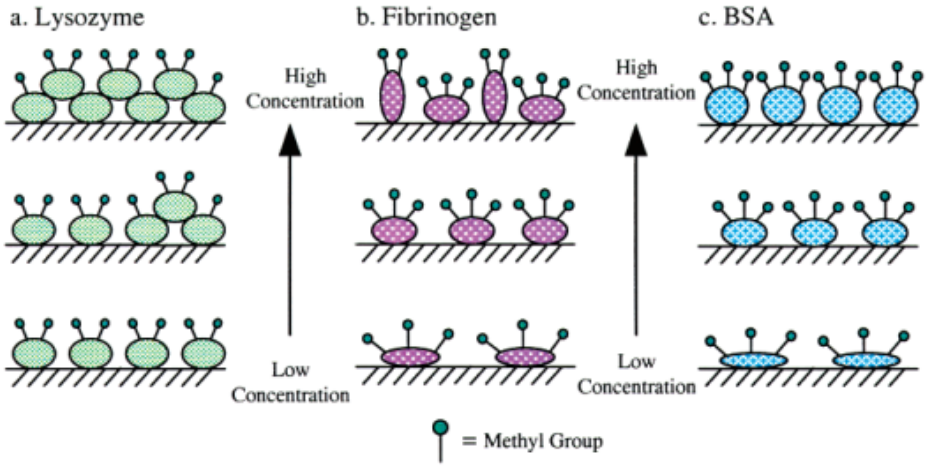

Figure 13. *Diagram illustrates different spreading tendencies of soft proteins (Fibrinogen and BSA) and hard one (Lysozyme) and effect of bulk concentration of protein stock (Kim & Somorjai 2003).*

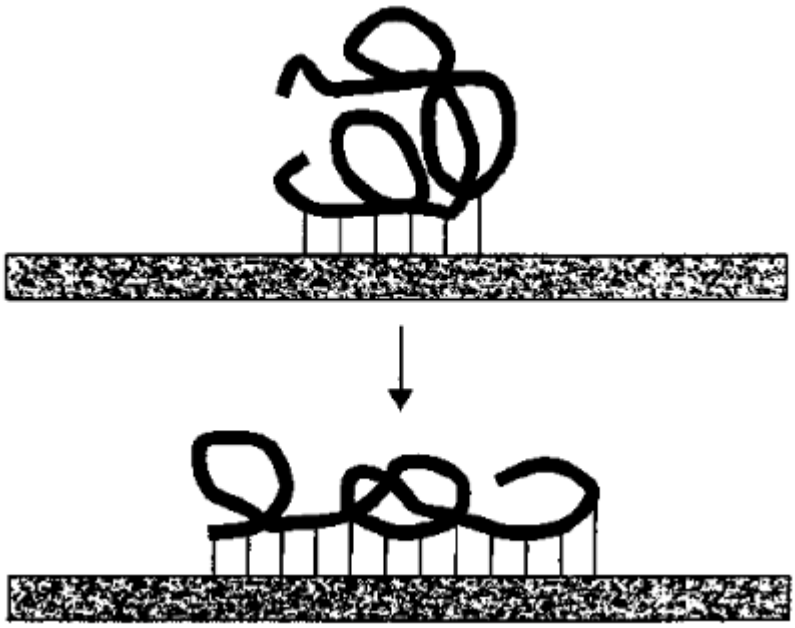

Figure 14. *Diagram of protein unfolding and spreading movement upon adsorption (Dee et al. 2003).*

3. RESEARCH METHODOGY AND MATERIALS

This part describes the glass processing as well as the surface treatments performed to modify the glass surface. The glass surface properties were studied by contact angle and Fourier transform infrared spectroscopy. The impact of the surface modification on protein adsorption was evaluated using two model proteins, i.e. fibronectin and albumin. Finally, the impact of fibronectin at the surface of the glass on the early cell attachment and proliferation was investigated.

3.1 Glass formation

Glasses of five different compositions were produced using traditional melting method. Silica-based bioactive glasses – S53P4 and 13-93 – were prepared using analytical grade SiO_2, Na_2CO_3, $(CaHPO_4).2H_2O$, $CaCO_3$, K_2CO_3, MgO, as raw materials. The other three glass compositions belong to novel phosphate-based glasses family, whose compositions were developed based on Sr50 glass and doped with different metallic oxides M_xO_y into its formula as following $[x(M_xO_y) – (100 – x)(0.5P_2O_5 – 0.2CaO – 0.2SrO – 0.1Na_2O)]$ (Mishra et al. 2017). To produce phosphate glasses, analytical grade $CaCO_3$, $SrCO_3$, $NH_4H_2PO_4$, $Na(PO_3)$ were used as raw materials and CuO, Fe_2O_3, Ag_2SO_4 as the precursors of metallic oxides. $Ca(PO_3)_2$ and $Sr(PO_3)_2$ were prepared beforehand as a result of the reaction between carbonates and $NH_4H_2PO_4$ at an elevated temperature as described in the previous work of Mishra et al. (2016). The nominal composition of these glasses is presented in the tables below.

Table 2. *Composition of silicate-based glasses (wt%).*

	SiO_2	Na_2O	P_2O_5	CaO	K_2O	MgO
S53P4	53.0	23.0	4.0	20.0	-	-
13-93	53.0	6.0	4.0	20.0	12.0	5.0

Table 3. *Composition of phosphate-based glasses (mol%).*

	P_2O_5	Na_2O	CaO	SrO	CuO	Fe_2O_3	Ag_2O
Cu4	49.0	9.8	19.6	19.6	4.0	-	-
Fe2	49.0	9.8	19.6	19.6	-	2.0	-
Ag2	49.0	9.8	19.6	19.6	-	-	2.0

Ingredients were weighted, crushed using a porcelain mortar and pestle and mixed well to create a relatively fine and uniform mixture. It was then transferred to a crucible, which was either quartz – for phosphate-based glasses – or platinum – for silica-based glasses. The batch was then melted in an electric furnace (Nabertherm GmbH, Germany) and the melt was then cast into a preheated brass mold to obtain a glass rod of approximately 10 cm in length and a diameter of 12 mm. These glass rods were then annealed around 50ºC below their respective glass transition temperature – for 6 to 8 hours to eliminate internal thermal stress and then let cool to room temperature.

Glass rods were cut into disks of 2 mm in thickness. These disks were then wet polished using sand papers of 400 – 4000 grit sizes.

3.2 Surface treatment

Polished glass disks were divided into three groups – each underwent a washing step with either one of three buffer solutions of three different pH values: acidic 5.0; neutral 7.4 and basic 9.0. Buffer solutions were prepared using Tris-HCl (neutral and basic) or Citric acid-Sodium citrate (acidic), filtered through 0.2 µm filter paper and autoclaved before used. All buffer solutions had an ionic concentration of 10mM. Prior to washing in buffer solutions, samples were washed in acetone-water solution (95% v/v) in ultrasonic bath for 5 minutes to eliminate contaminations. Samples were washed three times, each time in 150 ml of buffer solutions – 5 minutes in ultrasonic bath. They were then left to dry in a laminar hood for 24 hours.

Following the washing step, half of the samples were functionalized using 3-aminopropyltriethoxysilane (APTES, 98% Alfa Aesar). Samples were marked on one surface and only the other intact surface was used for further analysis. A batch of 9 washed samples were placed into a 400ml beaker (Duran Schott, d = 80mm) so that the intact surface was facing upward. A solution of 150 ml of ethanol 96% and 70 µL APTES was gently added to the beaker. Samples were drained after 6 hours of immersion at room temperature and then dried, in an oven, at 100ºC for 1h to finalize the reaction as well as consolidate the silanization coating layer. After that, samples were washed with ethanol by sonication for 5 minutes to remove excessive and unbound silane and again dried at 100ºC for 1 hour. Silanized samples were stored in a desiccator.

From this point on, a labelling system has been established to distinguish samples that underwent different treatments (Figure 15 and Table 4).

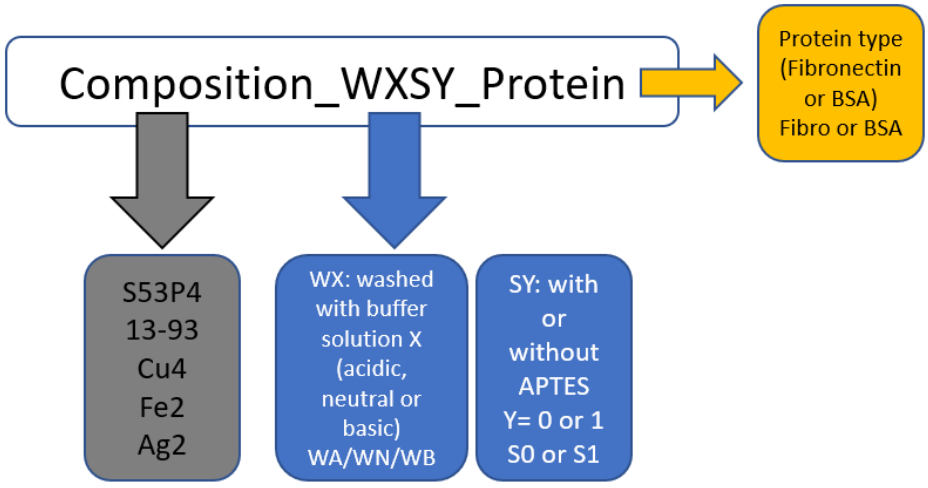

Figure 15. *The labelling system for samples undergoing different treatments.*

Table 4. *Full description of all sample names.*

Treatment		Composition				
	Buffer solution	**S53P4**	**13-93**	**Cu4**	**Fe2**	**Ag2**
Washed	Acidic	S53P4_WAS0	13-93_WAS0	Cu4_WAS0	Fe2_WAS0	Ag2_WAS0
Washed & Silanized	Acidic	S53P4_WAS1	13-93_WAS1	Cu4_WAS1	Fe2_WAS1	Ag2_WAS1
Washed	Neutral	S53P4_WNS0	13-93_WNS0	Cu4_WNS0	Fe2_WNS0	Ag2_WNS0
Washed & Silanized	Neutral	S53P4_WNS1	13-93_WNS1	Cu4_WNS1	Fe2_WNS1	Ag2_WNS1
Washed	Basic	S53P4_WBS0	13-93_WBS0	Cu4_WBS0	Fe2_WBS0	Ag2_WBS0
Washed & Silanized	Basic	S53P4_WBS1	13-93_WBS1	Cu4_WBS1	Fe2_WBS1	Ag2_WBS1
Untreated	-	S53P4_Un-treated	13-93_Un-treated	Cu4_Un-treated	Fe2_Un-treated	Ag2_Un-treated

The abbreviation for the protein species used in the grafting experiments is the last component of the labelling system, which could be either BSA (for Bovine Serum Albumin) or Fibro (for Fibronectin) or Ref – indicating that the sample had no proteins on the surface and was only used as a negative control.

3.3 Surface characterization methods

Static contact angle measurements were performed on both untreated and treated samples using sessile droplet method on Attension Theta contact angle meter (Biolin Scientific) to examine the effects of treatments on the wettability of the samples. A droplet of 2-3

µL of the corresponding buffer solutions was set onto the surface of bioactive glass disks and the image of the droplet was recorded with a high-speed camera. Contact angle values of both left and right sides of the droplet were measured using the software Attension Theta (Biolin Scientific). Figure 16 shows an example of contact angle measurement on a S53P4 bioactive glass disk. The measurements were performed in triplicates, i.e. 3 measurements on 3 disks, for each category to get the average and standard deviation values.

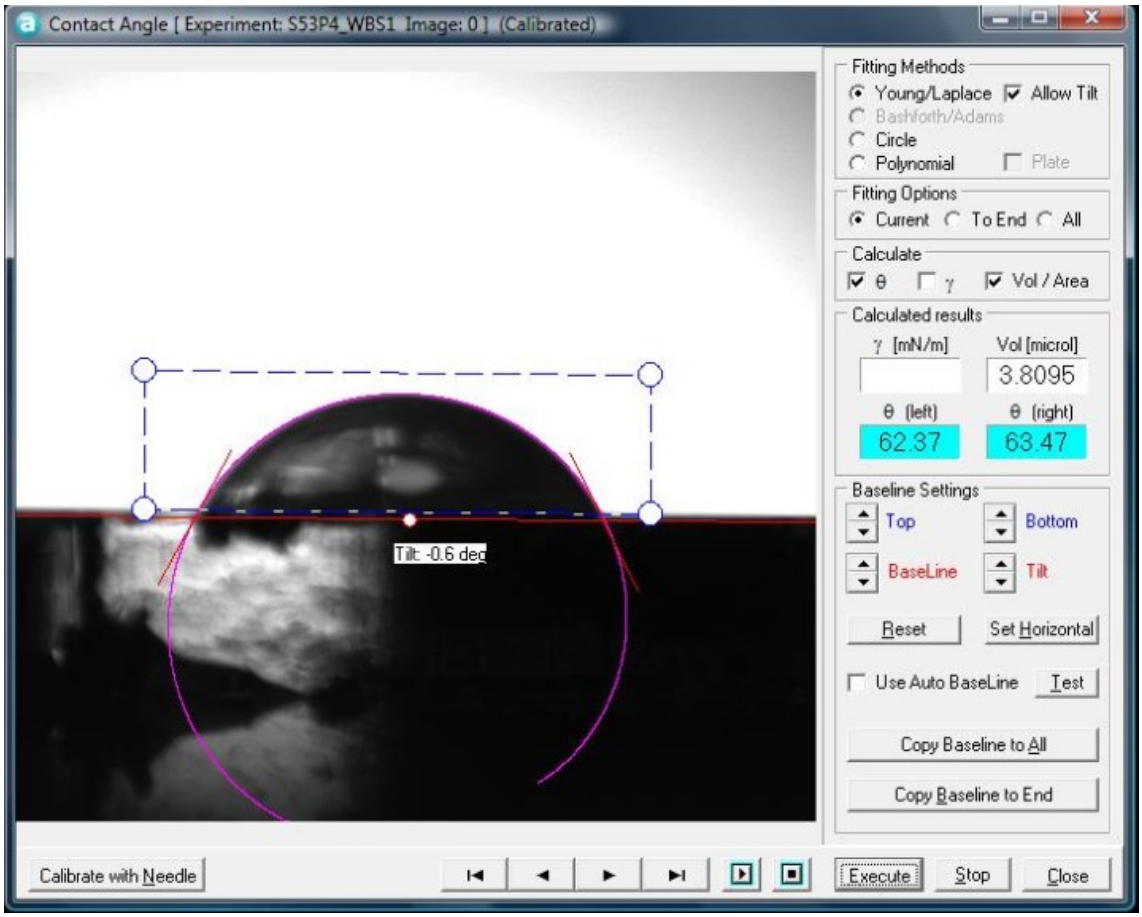

Figure 16. *Contact angle values of S53P4 glass disc measured using Attension Theta software.*

Changes in the glass surface chemistry were investigated using Fourier-transformed infrared spectroscopy (FTIR) in Attenuated Total Reflectance (ATR) mode on solid glass disks. Infrared (IR) spectra of untreated and treated glass disks were recorded on Spectrum One Perkin Elmer spectrometer within the 4000 – 600 cm^{-1} range with 1 cm^{-1} resolution. All spectra were background corrected and normalized to the peak with maximum intensity.

3.4 Protein attachment

Treated samples were grafted with fluorescent labelled Bovine serum albumin (BSA) and Fibronectin and subsequently imaged under confocal fluorescence microscope for confirmation of protein presence. BSA (Sigma-Aldrich, lyophilized, ≥96%) and Fibronectin (purified from human plasma using gelatin column by Protein Dynamics Group – Bio-MediTech) were labelled with Alexa Fluor™ 488 NHS Ester (ThermoFisher Scientific) with 1.04 and 8.07 dyes/protein, respectively.

Proteins were diluted to obtain a protein solution concentration of 10 µg/mL using the buffer solutions from the previous washing step. Protein grafting took place on Polystyrene (PS) uncoated 6-well plates. A pair of 120µm-thick polydimethylsiloxane (PDMS) strips were laid on PS surface to provide sufficient space (area of 80 – 90 mm^2 – thickness of 120 µm) for protein solution to reside in without being compressed by the weight of bioactive glass disks and achieve uniform protein density. Samples were placed on the spacers (PDMS strips) in contact with 20 µl protein solution (of the corresponding buffer solution used in the washing step) for 30 minutes. Bioactive glass disks were then washed 3 times, each time for 2 minutes using orbital shaker at a speed of 250 rpm, with 2ml of PBS 1X in the well plate to remove loosely bound protein.

Samples were then removed from PBS, dipped through deionized water a few times and immediately mounted on glass slides with 10 uL of ProLong™ Diamond Antifade Mountant (Invitrogen™, ThermoFisherScientific) to preserve the fluorescence properties of the dyes. Mounted samples were covered and stored at room temperature in a dark place for at least 24 hours to completely cure before being imaged for fluorescence microscopy.

3.5 Image analysis of protein grafted samples

Samples grafted with proteins labelled with fluorescence dye Alexa Fluor™ 488 were imaged under confocal fluorescence microscopes after 24 hours of curing to examine the overall coverage of protein on bioactive glass substrates. Due to technical issues, BSA grafted and Fibronectin grafted samples were imaged under 2 different microscopes (Carl Zeiss LSM 780 and Nikon A1R+) and different configurations in terms of magnification and immersion medium, thus the comparisons were only made among those images achieved from the same microscope to ensure the rationality of the results. The imaging procedure was, however, similar: the protein grafted surface of the bioactive glass disks was located first by focusing on the disks' edge and the green fluorescence signals on the sample surface were recorded. Recorded images could include a stack of multiple z planes (total thickness of a few micrometres) to ensure the best signals and partly compensate for the tilting surface of the glass disks, if applicable. The BSA grafted samples were imaged on Carl Zeiss LSM 780 with magnification of 25x using oil immersion while

Fibronectin grafted ones were imaged with 20x objective lens in air (no immersion medium was used). The average fluorescence intensity data were extracted using ImageJ software as an attempt to quantify the overall coverage of protein on sample surface.

3.6 Cell culture

The improvement of protein adsorption by surface treatments on bioactive glasses were correlated to the adhesion and spreading of Mouse Embryonic Fibroblasts (MEFs). To reduce the workload for this stage, we chose 3 compositions of bioactive glass, namely S53P4 (silica-based), Ag2 and Sr50 (phosphate-based) and the best surface treatment from previous protein adsorption analysis. MEFs were cultured on untreated, basic washed and silanized samples with or without Fibronectin coating prior to cell plating.

Bioactive glass disks were fixed to the glass coverslip bottom of a 12-well plate (MatTek Corporation, USA) using polystyrene (PS) liquid glue (made by dissolving rigid PS in xylene and drying via solvent evaporation mechanism) and sterilized under UV light for 1 hour. Regards dimensions, bioactive glass discs (12 mm in diameter) were glued to the cover glass (14 mm in diameter) at the bottom of each well (bottom internal diameter 22.09 mm).

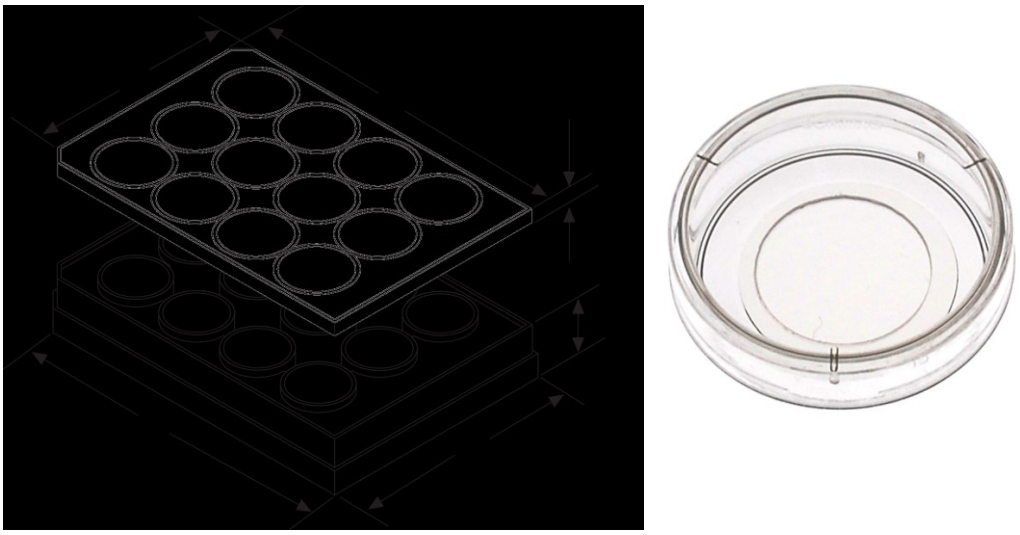

Figure 17. *Dimensions of the 12-well plate (left) and structure of each well (right). (Images from MatTek Corporation).*

Normal borosilicate glass coverslips were used as positive reference to ensure a healthy population of MEFs. The cell culture experiments were conducted in a layout as illustrated in table 4 below and all conditions and compositions were tested in the same round. The experiments were repeated at the minimum 3 times.

Table 5. *Layout for cell culture tests.*

Composition	Condition			
	S53P4_Untreated	S53P4_WBS1	S53P4_WBS1_Fn	NormGlass
	Ag2_Untreadted	Ag2_WBS1	Ag2_WBS1_Fn	NormGlass_Fn
	Sr50_Untreated	Sr50_WBS1	Sr50_WBS1_Fn	-

Fibronectin was deposited prior to the cell plating at the concentration of 10µg/mL in PBS for 1 hour at 37ºC. The whole plate was then sterilized under UV light for 1 hour. MEFs were trypsinized from the culture flask, passed to a new cell culture medium, checked for cell density and diluted to the concentration of 50.000 cells/mL or roughly 13.000 cell/cm^2. Cell culture medium is a mixture of the DMEM with GlutaMAX™-I (LifeTechnologies) supplemented with additional 10% Foetal Bovine Serum, 1% penicillin/streptomycin (antibiotic). Each well was filled with 1ml of cell suspension and after 2 hours of incubation, they were live-imaged using EVOS FL cell imaging system (LifeTechnologies) for 18 – 20 hours. For each well, five beacons, i.e. points for imaging, were chosen and imaged under 20x objective every 5 minutes.

After the EVOS live imaging session, the medium was removed, cells on bioactive glass samples were fixed and preserved using fixative solution which was 1X PBS containing 4% paraformaldehyde (PFA) at 37ºC for 15 – 30 minutes. The fixative solution was then removed and permeabilization buffer solution, which was 0.2% Triton (Sigma-Aldrich) in 1X PBS, was added to the well and incubated for 5 minutes to allow staining agents to later infiltrate the cell membranes. After that, cells were incubated for another 30 minutes in blocking buffer solution to avoid non-specific binding of staining antibodies. Cells were then treated with with α-paxillin and goat anti-mouse antibodies (Alexa Dye 568 red) to recognize their focal adhesions as well as stained with phalloidin (Alexa Dye 488 green) to identify actin filaments. Samples were mounted with ProLong™ Gold Antifade Mountant (Invitrogen™, ThermoFisherScientific) containing blue DAPI to highlight the nuclei. Samples were allowed to cure for 24 hours at room temperature in the dark before being imaged with Nikon A1R+ fluorescence confocal microscope.

4. RESULTS AND DISCUSSION

In this part, the results on the impact of various surface treatments on the glasses' ability to immobilize protein are discussed. Washing of the samples was done using acid, neutral or basic buffer solution. Half of the samples were further silanized using APTES. The wettability of the samples prior washing, after washing and after silanization was studied by contact angle measurements. Contact angle data is also capable of giving an indication of the proper silanization of the samples. The change in surface chemistry induced by the surface modification steps was assessed by FTIR. Later, protein (albumin and fibronectin) adsorption at the surface-modified glasses was evidenced using fluorescently labelled proteins. Finally, the cell culture tests were done to confirm the effects of improved protein adsorption on cell adhesion and proliferation.

4.1 Material and treatment characterization

4.1.1 Contact angle

The contact angle data were collected to assess the effect of various surface modifications on the surface wettability. Contact angle can also provide the evidence of a successful APTES grafting on bioactive glasses surface (Massera et al. 2016). All investigated glasses naturally exhibited very hydrophilic surfaces. As prepared, the contact angle of all the polished surfaces was lower than 20^{o}, with the exception of 13-93 glass, which exhibited contact angle of 34 ± 7^{o}.

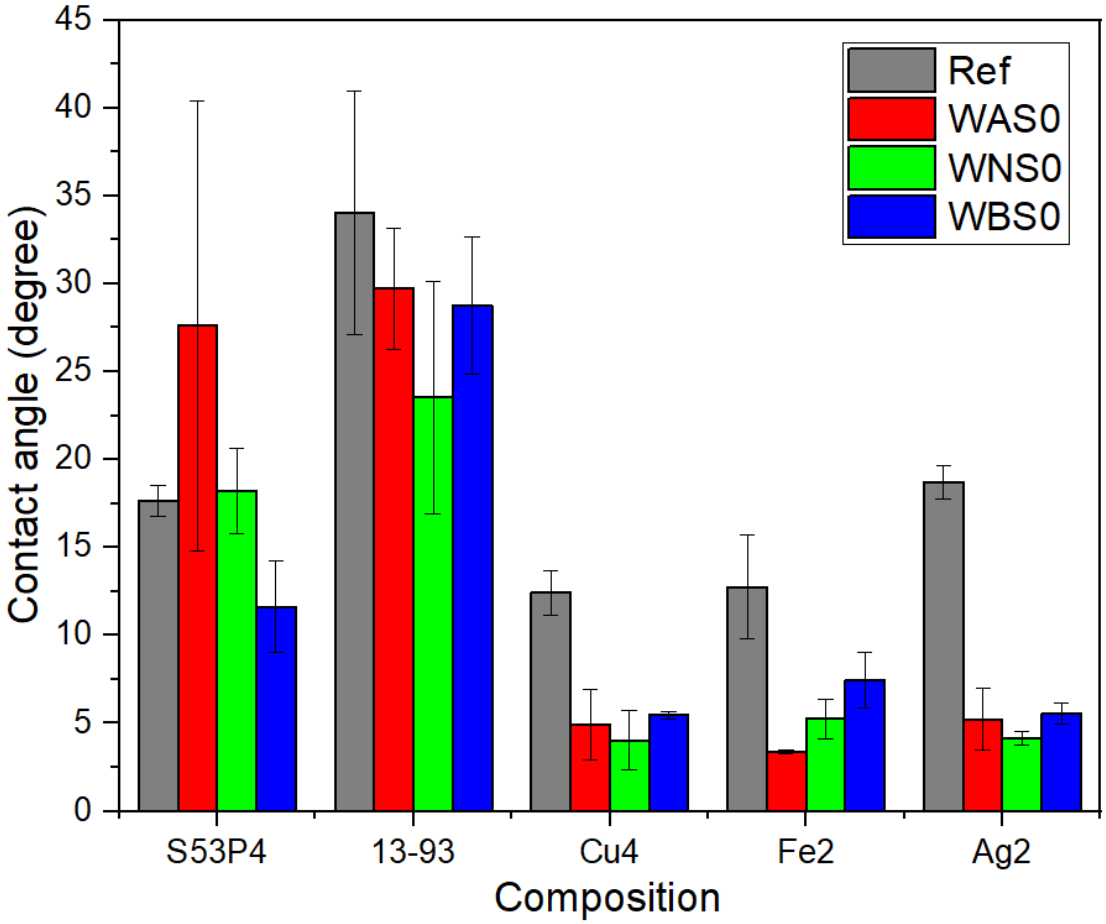

Figure 18. *Effect of washing treatments on wettability of the five compositions.*

Figure 18 presents the contact angle measured at the surface of bioactive glasses washed in various buffer solutions in comparison with the untreated glass ones. Washing bioactive glass discs with different types of buffer solutions caused a slight change in contact angle. In the case of the three phosphate glass compositions, washing of the glass surface, regardless of the buffer solution pH, led to a decrease in the contact angle. This could have been anticipated. It is reported in a study in 2016 by Massera et al. that washing the phosphate glass surface increases the exposure of OH groups which would induce an increased wettability of the surface. However, in the case of the silicate glasses such trend was hardly seen, despite being also reported in the same literature when using ethanol/DI water as washing solution (Massera et al. 2016). In this study, while a slight decrease in the contact angle could be reported for the glass 13-93, it is apparent that washing the glass S53P4 with an acidic buffer solution led to an increase in contact angle. The glass S53P4 only exhibited a decrease in the contact angle when the surfaces were washed with a basic buffer solution.

The significant differences between the contact angle change on silicate and phosphate bioactive glasses, and even more so between the two silicate bioactive glasses could be related to drastic change in the glass surface chemistry. Silicate bioactive glasses exhibit

a non-congruent dissolution thereby the alkaline and alkaline earth ions leach out at faster rate than the glass forming ions. Such non-congruent dissolution leads to significant compositional change at the glass surface post-immersion in aqueous medium. Phosphate bioactive glass, however, exhibit a congruent dissolution, thereby all ions leach out at the same rate. Such dissolution leads to an unchanged surface chemistry upon dissolution. It is also common knowledge that the glass 13-93 is more stable in aqueous solution than the glass S53P4 (Massera et al. 2016).

Figure 19 presents the effects of the silanization treatment on the contact angle depending on the pH of the washing solution used. In all cases the silanization steps led to a remarkable increase in contact angle when compared to the washed surface. As reported by Massera et al. (2016), an increase in the contact angle upon silanization can be considered as a sign of proper silane grafting at the glass surface. Indeed, the APTES layer converts the hydrophilic surface of bioactive glasses into a more hydrophobic one.

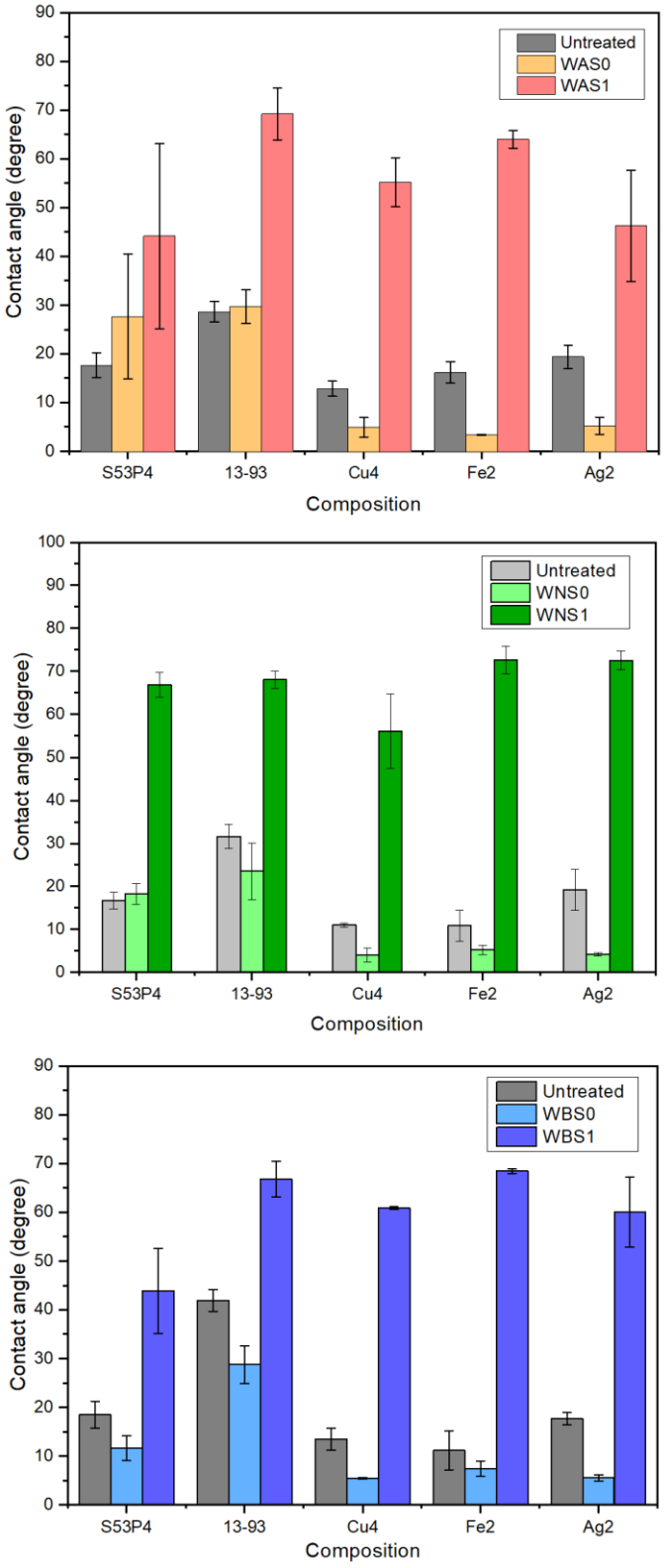

Figure 19. *Effects of silanization treatment on contact angle data. From top to bottom: acidic washed, neutral washed and basic washed.*

The contact angle data gave the first base to predict the prospects of protein adsorption capacity of our glasses after experiencing different treatments, especially in silanized samples. Many studies suggest that hydrophobic surfaces usually attract more proteins to

the surface although the orientation of proteins might not be as highly ordered as in hydrophilic surfaces (Kim & Somorjai 2003). Therefore, it was expected that silica-based glasses, especially 13-93, would exhibit higher amount of proteins on the surface in subsequent imaging analysis of fluorescently-labelled proteins. On the other hand, although APTES grafting caused a decrease in wettability, it is believed that their explicit surface chemistry could promote protein adsorption.

4.1.2 FTIR

To get a better understanding of the impact of surface treatment on the surface chemistry, ATR-FTIR spectra were recorded after each step. All spectra were background corrected and normalized to the peak with maximum intensity.

The spectra of S53P4 glass samples undergoing various surface treatment are presented in figure 20 and 21.

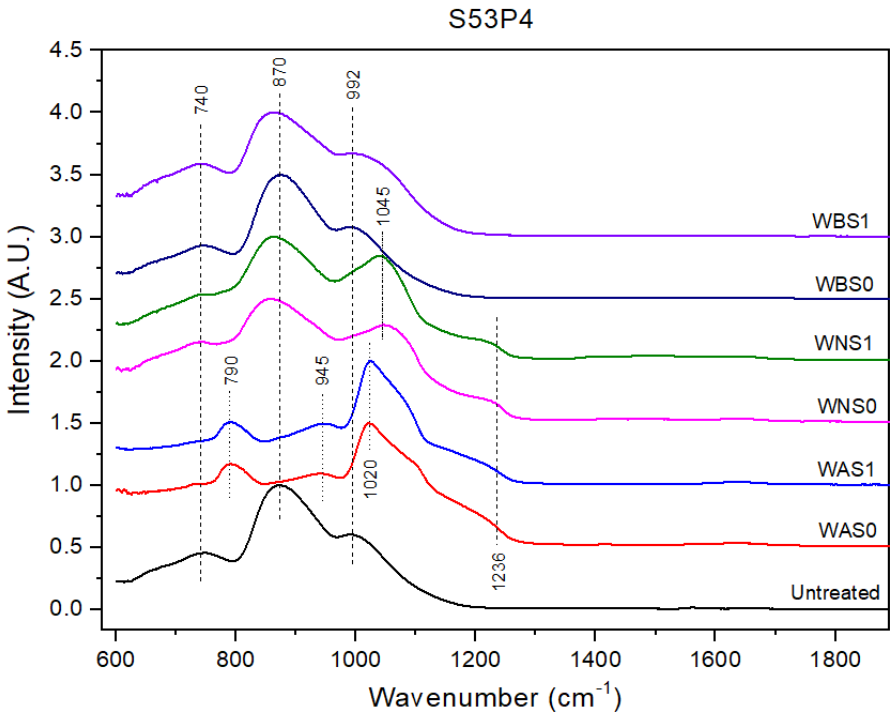

Figure 20. *FTIR spectra of S53P4 glass in 600 – 1800 cm^{-1} region.*

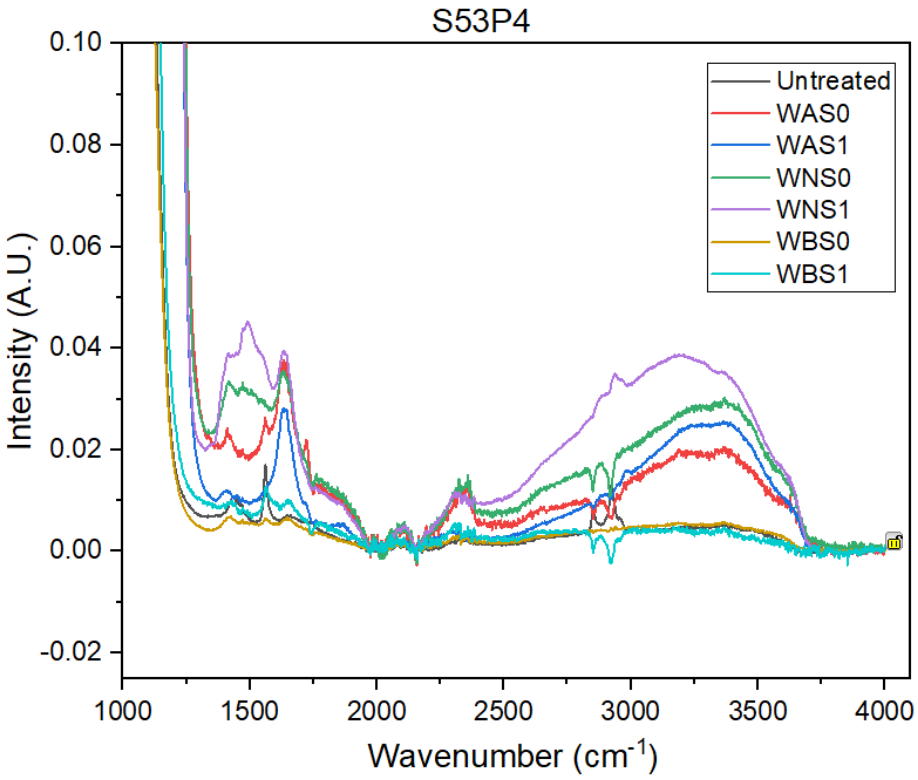

Figure 21. *FTIR spectra of S53P4 glass in 1000 – 4000 cm^{-1} region.*

For S53P4 silicate glass, the spectra of untreated samples feature 3 absorption bands in at 740, 870 and 992 cm^{-1} that could be assigned to Si–O–Si bending, Si–O–Si symmetrical stretching mode and Si–O–NBO vibration, respectively (Serra et al. 2003, Magyari et al. 2015). On the other hand, samples washed in buffer solutions show changes in their surface chemistry as the positions and intensities of the absorption bands vary with different pH values.

While the basic treated S53P4 samples show no significant changes in surface chemistry compared to as-prepared glass, there is a broadening of all three bands upon silanization which could be attributed to either the silane layer deposition or to the leaching of the cation which could lead to empty space around the silica network. Their spectra also feature very little trace of surface hydration, i.e. the large band of O–H stretching at 3000-3600 cm^{-1}, that is largely observed in other conditions.

Samples washed in neutral buffer solution (WNS0 and WNS1) show some remarkable deviations from the reference (untreated) sample in both overall spectral shape, position and strength ratio of the featuring absorption bands in 600 – 1300 cm^{-1} region. The absorption band at 740 cm^{-1} is detected but with weaker signal and the band originally assigned for Si–O–Si symmetrical stretching mode in reference sample slightly shift from 870 cm^{-1} to lower frequency 860 cm^{-1}. The most interesting feature of those samples treated under this condition is the rise of a new band at 1045 cm^{-1} which is almost as strong as the main band at 860 cm^{-1}. This new band could be attributed to P–O vibration

mode arising from the formation of carbonated hydroxyapatite (HCA) (Li et al. 2007). A small shoulder also appears at 1236 cm^{-1} in the spectra of these samples as well as in acidic washed samples. This could be assigned for Si–O–Si symmetrical stretching which has been reported as a sign of the formation of a silica-rich layer during the glass dissolution (Brentrup et al. 2009, Massera et al. 2012).

The spectra of samples washed in acidic solutions are significantly different from the untreated samples, with 3 main bands detected at frequencies other than those reported for the base-glass as well as a new shoulder at 1236 cm^{-1} as mentioned in neutral washed samples. The band at 740 cm^{-1} diminishes to almost undetectable while another band rises next to it at 790 cm^{-1}. The later band and the shoulder at 945 cm^{-1} corresponds to the C–O vibration mode in CO_3^{2-} (Saiz et al. 2002). They, together with the strong band at around 1020 cm^{-1} attributed to P–O in PO_4^{3-}, are the evidence for the formation of carbonated hydroxyapatite (HCA) on the surface of acidic washed samples (Li et al. 2007, Saiz et al. 2002).

Besides the main bands in the region 600 – 1300 cm^{-1}, there are a few more minor bands appearing in the spectra of neutral and acidic washed samples in the range [1400 - 1500] cm^{-1}, approximately at 1413 cm^{-1} and 1493 cm^{-1}, which have been reported to be associated with carbonate group (Massera et al. 2012) (Figure 21). The spectra of these samples also feature an absorption band at 1632 cm^{-1} and a broad band in the range [3000 - 3600] cm^{-1}, which could be assigned for O–H bending and stretching, respectively (Stuart 2004, pp. 97). In contrast, these bands are completely absent from the spectra of basic treated samples. This proves that neutral and acidic washing treatments result in a high degree of surface hydration while basic treated samples feature very little surface hydration.

In general, it is apparent that decreasing pH value of washing buffer solutions leads to an increase in the rate of the remineralization reaction. Meanwhile, samples washed in basic buffer solutions remain similar to untreated samples in their surface chemistry and very low degree of HCA formation and surface hydration was recorded.

Regards the effects of APTES coating treatment, it is difficult to detect any difference between samples with and without the silanization treatment. No conclusive distinction is detected in APTES coated samples considering those bands that are typically assigned to signature chemical bonds in APTES such as NH_2 in the range [2850 - 2900] cm^{-1}. The APTES coating layer on top of the surface might be too thin to be detected by a mono-reflection ATR cell.

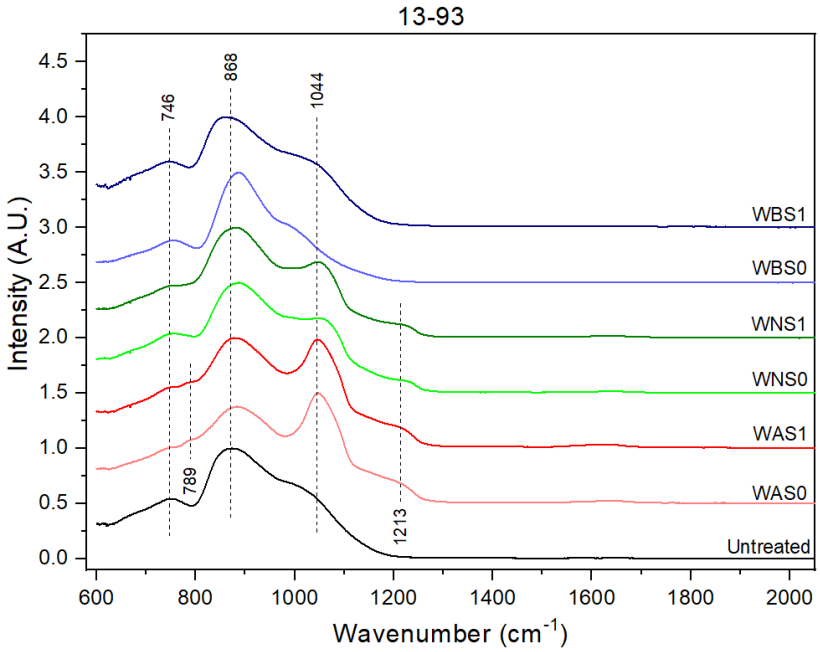

Figure 22. *FTIR spectra of 13-93 glass in 600 – 2000 cm^{-1} region.*

The spectra of 13-93 samples in Figure 22 also show similar patterns of surface chemistry changes over different conditions as S53P4 glass. In basic condition, almost no change could be detected. In neutral condition the band assigned to Si–O–NBO (at 1044 cm^{-1}) increases in intensity at the expense of the Si–O–Si vibration (at 868 cm^{-1}), while the shoulder at 1236 cm^{-1} assigned to Si–O–Si in Q_4 units arose. As previously discussed, this indicates that the glass as started to dissolve, and the silica rich surface started to repolymerize. However, when compared to the glass S53P4 the changes are less pronounced. This is simply due to the the lower dissolution rate of the glass 13-93 and therefore indicates that the dissolution process is only starting. In acidic condition, the premises of the phosphate vibration start to be seen, but as opposed to the FTIR spectra of the glass S53P4, were a clear HA layer was formed, here the layer is only initiating to precipitate and is not yet well formed.

The 3 compositions of phosphate-based glasses exhibit similar FTIR spectra for different treatments where all the main bands in the range 600 – 1500 cm^{-1} feature characteristic bands of the phosphate glass network as explained thoroughly by Massera et al (2016). Figure 23 shows the spectra of Cu4 glass as an example for FTIR spectra of phosphate-based glasses after various treatments. Spectra of the other two compostitions could be found in the appendix. The overall spectral shape and position of the absorption bands also remain unchanged over different treatments. Spectra of all phosphate-based glasses show a dominant peak at 865 cm^{-1} which is assigned for P–O–P asymmetric stretching in Q_2 units; two bands at 708 and 782 cm^{-1} corresponding to P–O–P symmetrical stretching modes in metaphosphate network; a band peaking at 1078 cm^{-1} and a shoulder centered at 980 cm^{-1} possibly induced by stretching vibrations of Q_1 units and the last band at 1234 cm^{-1} as the representative for Q_2 units (Massera et al. 2013).

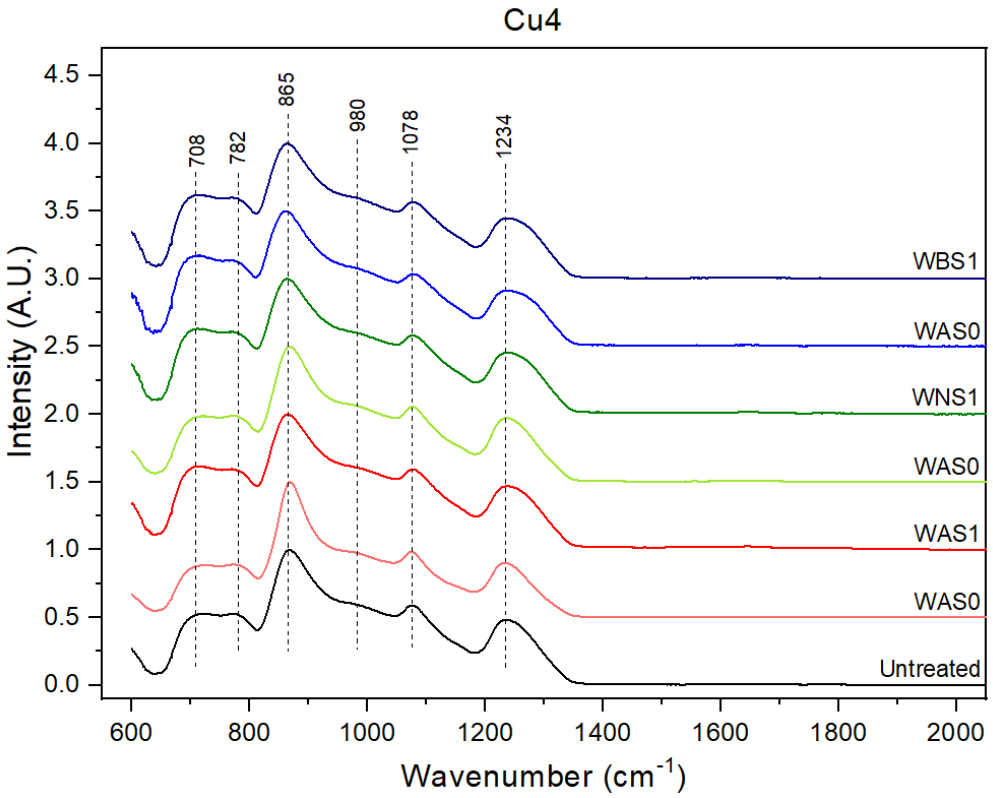

Figure 23. *FTIR spectra of Cu4 phosphate glass in the region 600 – 2000 cm^{-1}.*

4.2 Protein grafting effect

4.2.1 Confocal fluorescence microscopy

Here the fluorescence images recorded from confocal fluorescence microscope are presented as matrices to aid the comparison process. The green scale bar represents 100µm length in both sets of images (Figure 24 – 26 and 28 – 29). The green fluorescence signal of the images is correlated to the presence of proteins on bioactive glass disks in terms of

total coverage as well as signal intensities. The same laser power and signal amplification were used for all images taken on the same equipment to allow comparison.

Figure 24 presents the fluorescence images of BSA-grafted silica-based glasses experiencing different treatments. There was a remarkable contrast in fluorescence intensity between the surfaces with and without surface functionalization where stronger fluorescence signals were measured in all surfaces with APTES, suggesting more BSA were present there than on those without APTES. The signals were also stronger at the sites of topographical patterns such as grooves and scratches, which shows a tendency of proteins to accumulate at these sites.

Although very low fluorescence signals were recorded on S53P4 glass surfaces without APTES, they did feature a light coverage of fluorescence signal, perhaps a bit dim due to the low quality of compressed images. Figure 25 is the large fluorescence image of the acidic treated S54P4 sample without the silane coupling agent (S53P4_WAS0_BSA) as an example of such surfaces where one could see an even coverage of weak fluorescence signal. It is interesting to point out that the surface of the glass S53P4 post washing treatment with acidic buffer solution featured unusual topographical patterns – probably cracks or grain boundaries – as opposed to all the other silicate glasses surface treated with other medium. This unique topographical pattern observed only in acidic treated S53P4 samples agrees with the FTIR analysis and is likely a sign of the rapid formation of HCA layer in acidic environment.

A similar improvement could be observed in 13-93 glass where most of the signal recorded on surfaces without APTES came from the grooves and scratches while the silanized surface exhibited much stronger signals and a significant increase in the intensity was recorded on the whole surface, suggesting a better coverage of BSA. Moreover, the level of fluorescence intensity recorded on APTES coated 13-93 samples was higher than on the counterparts of S53P4 composition, indicating more APTES was deposited on the former than on the later. This also shows that 13-93 has better compatibility with APTES than S53P4.

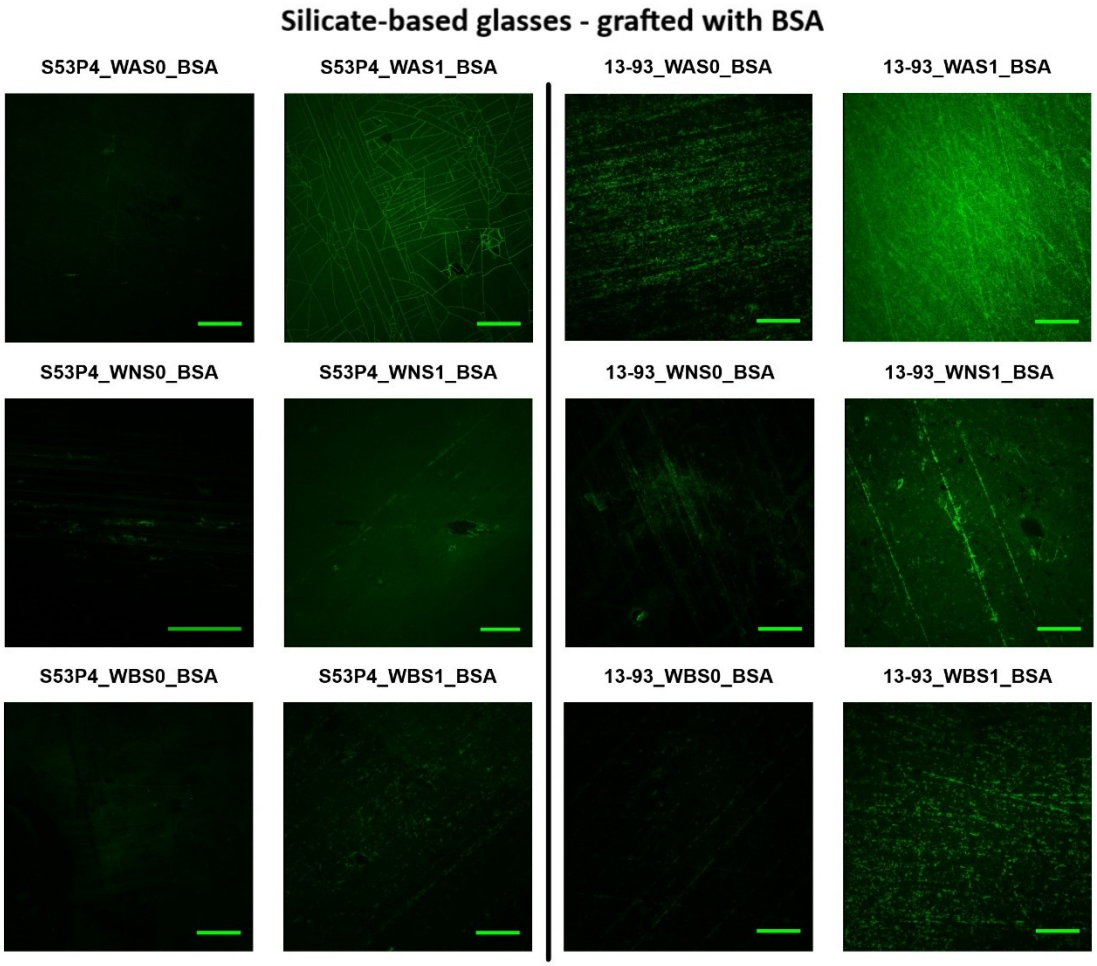

Figure 24. *Fluorescence images of BSA-grafted silica-based glasses. Equipment: Zeiss LSM 780. Scale bar represents 100 µm.*

Besides a clear contrast in samples with and without APTES, a comparison between different washing treatments and grafting conditions was also made to determine the most favourable treatments and grafting conditions for protein adsorption on the surface of bioactive glasses. It is important to point out again that the pH value of washing buffer solutions has a crucial effect on both proteins, e.g. positions of polar/non-polar or hydrophobic/hydrophilic groups, and bioactive glass surface, e.g. surface hydration and attraction of different electrolytes.

As the signals from samples grafted with BSA in acidic environment (pH = 5.5) were the strongest among the 3 conditions (acidic, neutral and basic), although the signals were dim in surfaces without APTES, BSA seemed to show a preference for this grafting condition.

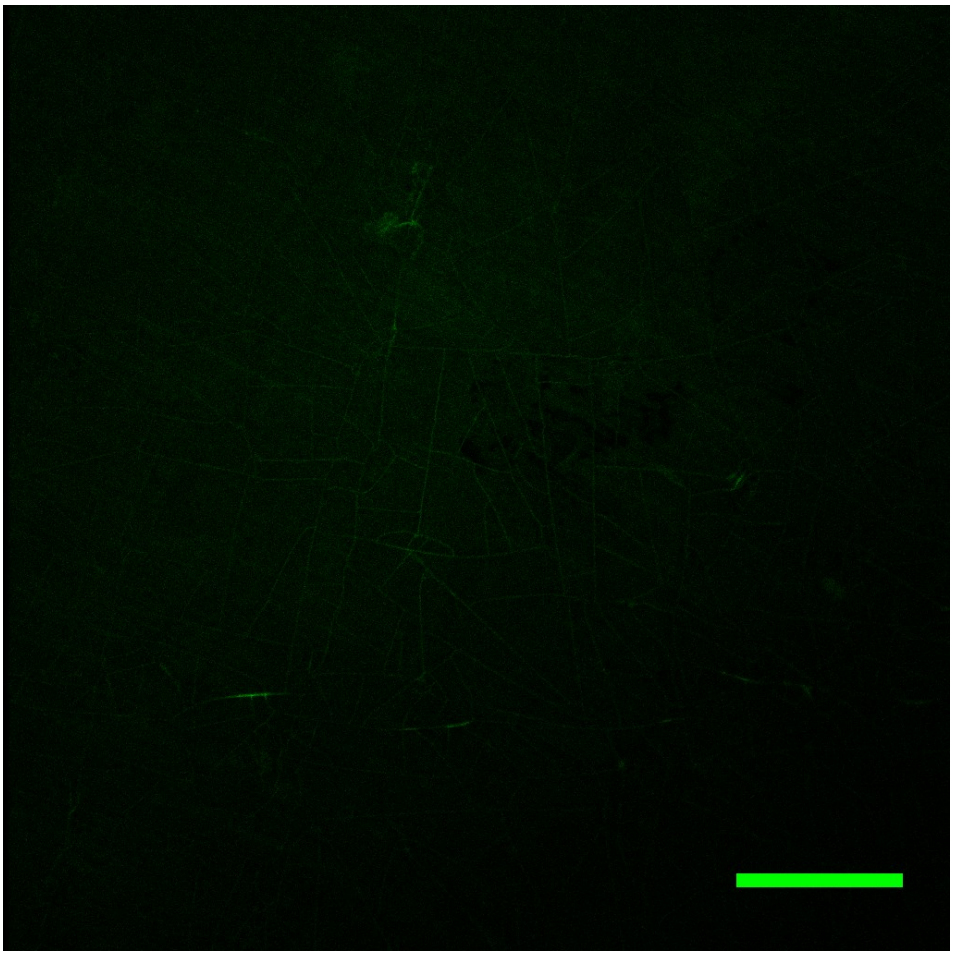

Figure 25. *Original fluorescence image of S53P4_WAS0_BSA. Equipment: Zeiss LSM 780. Scale bar represents 100 µm.*

The fluorescence images of phosphate-based glasses grafted with BSA are shown in figure 26. Almost no signals were recorded from washed phosphate glasses (no APTES), implying an inferior capacity of immobilizing BSA when comparing to the silica-based counterparts. Meanwhile, the APTES coating layer has significantly improved the BSA adsorption with an even layer of fluorescence signals detected and satisfactory overall coverage although the intensities were relatively lower than that of silica-based glasses, suggesting that their compatibility to APTES is lower than that of silica-based compositions.

Regards the effects of grafting environment, while one could comment that the acidic environment seemed to support BSA adsorption on Cu4 glass, the same conclusion could not be made for the other two glasses. The low signals of Fe2 samples cause difficulties in determining the best response among the 3 grafting conditions while the best signal for Ag2 glass was recorded on neutral washed sample where the BSA grafting took place in also neutral environment (Ag2_WNS1_BSA).

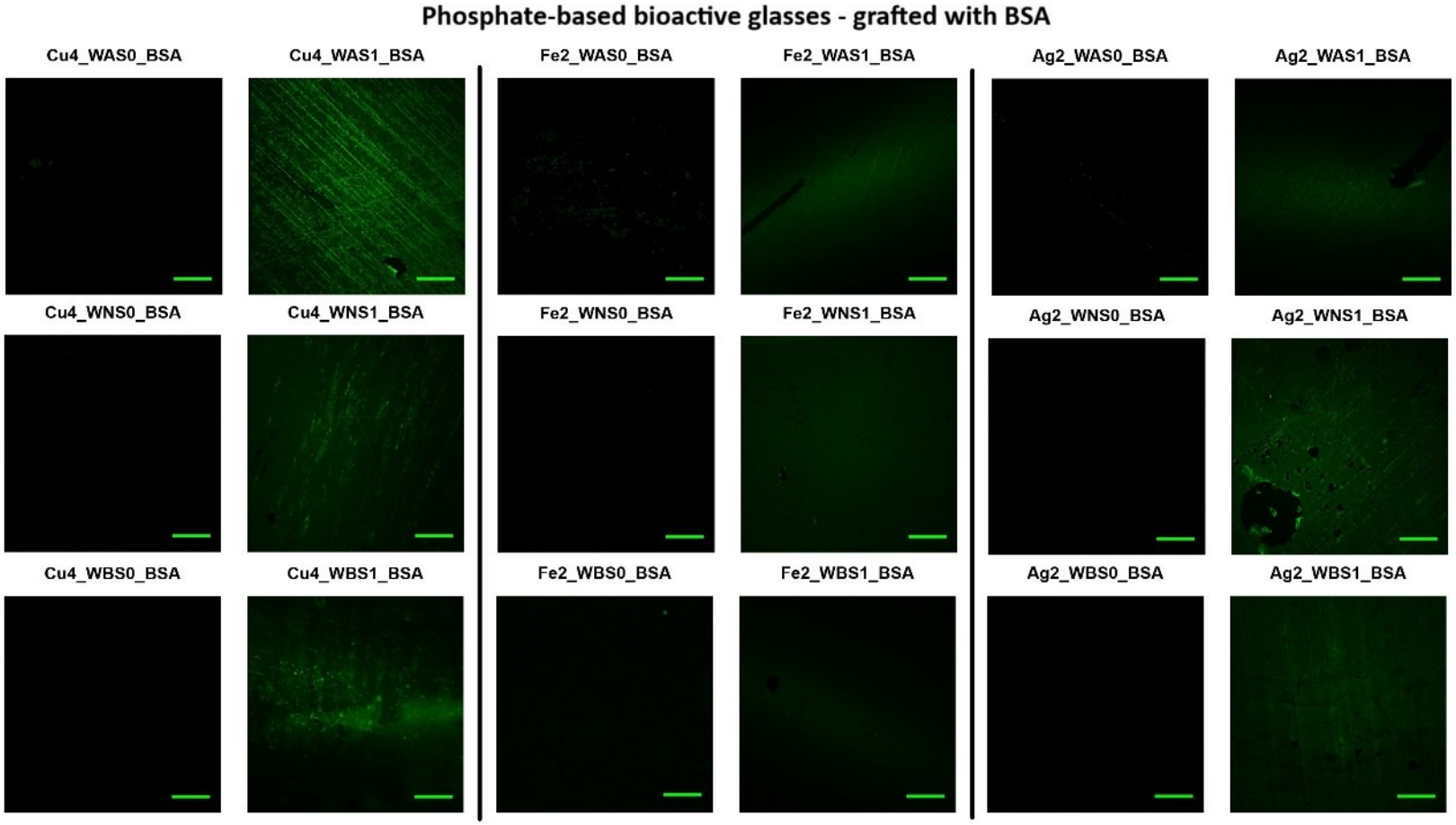

Figure 26. *Fluorescence images of BSA-grafted phosphate-based bioactive glasses. Equipment: Zeiss LSM 780. Scale bar represents 100 µm.*

As the visual evaluation was subjective, the average fluorescence signal intensities of the images were extracted using the software ImageJ and normalized to the intensity of acidic washed, silanized S53P4 samples with no proteins (Ref_S1 – Figure 27) to quantify the outcomes using ratiometric methods.

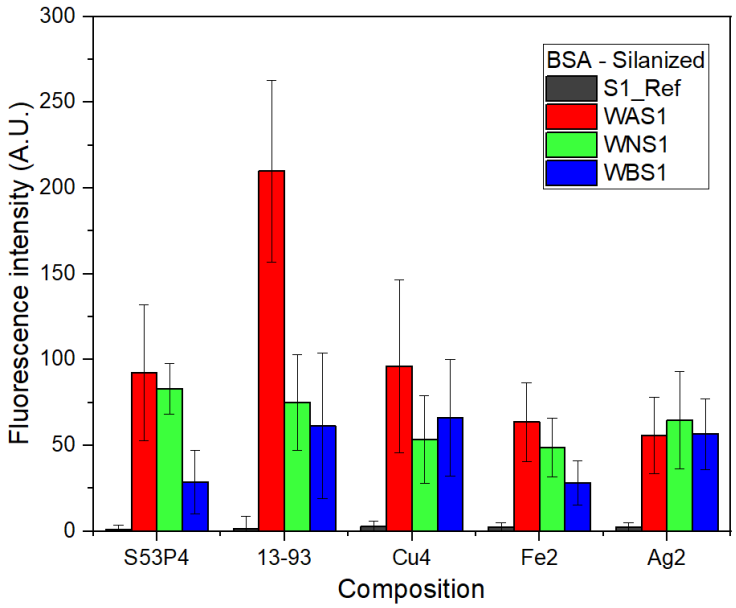

Figure 27. *Fluorescence intensity data of BSA-grafted samples with APTES coating, extracted using ImageJ software.*

The fluorescence intensity data obtained from ImageJ software were accompanied by a set of software-generated standard deviations which were quite high. However, these obtained fluorescence intensity data seem to support the visual evaluation as the highest intensities were observed in acidic washed samples (except for Ag2) where BSA was grafted in acidic solutions.

In general, the BSA grafting experiments and fluorescence images of all the samples confirm the beneficial effect of APTES in promoting BSA immobilization via chemical compatibility, the extent of which varies depending on the affinity of the glass composition towards APTES, i.e. the amount of APTES deposited on the surface of the glass under the same silanization condition. The proteins seem to assemble themselves into a uniform layer on samples coated with APTES instead of scattering in grooves and scratches on those without the APTES treatment. Acidic environment seems to favor BSA adsorption when high level of fluorescence intensity was detected in most of these cases compared to other grafting environments. Among 5 compositions, the silanized 13-93 sample grafted with BSA in acidic environment exhibited the strongest fluorescence intensity, which could be the synergistic results of the high concentration of APTES and the low pH environment.

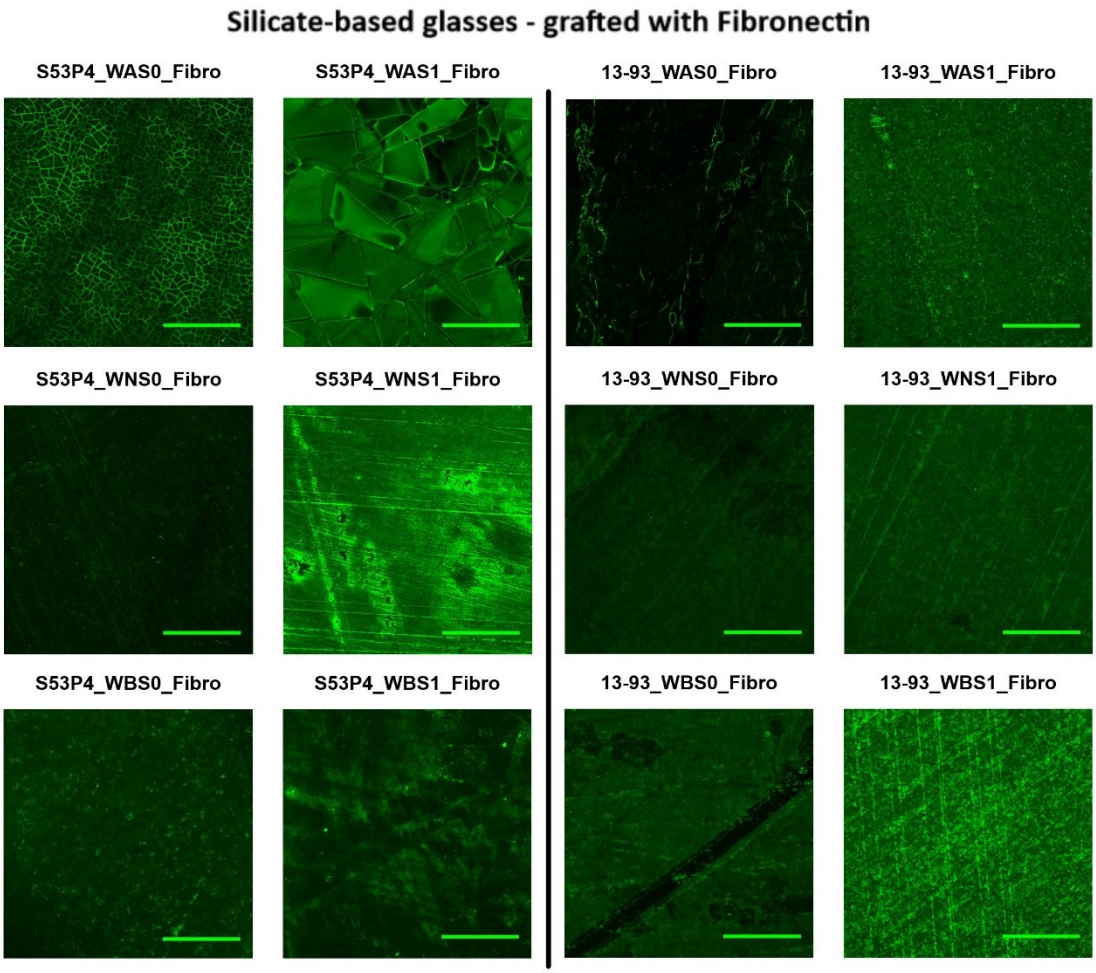

Figure 28. *Fluorescence images of Fibronectin-grafted silica-based glasses. Equipment: Nikon A1R+. Scale bar represents 100 µm.*

The fluorescence images of fibronectin-grafted silica- and phosphate-based samples are presented in figure 28 and 29, respectively. Here the signals were much stronger, especially on silicate glasses without APTES, thus giving a better basis for comparison and conclusion on the effects of washing treatments and pH value of protein solutions. Images of silica-base samples grafted with fibronectin in figure 28 show a similar effect of the APTES coating in improving fibronectin density present on the glass. Another worth noticing point is the development of unusual topographical patterns on acidic treated S54P4 samples which has been observed in the previously analyzed images of BSA grafted samples.

An increase in fluorescence signals was also recorded when increasing the pH value with the strongest signals observed on basic treated samples, suggesting basic environment (pH = 9.0) to be the most favourable grafting condition for fibronectin. However, an abnormally strong signal was seen on the APTES coated S53P4 sample that was grafted with fibronectin in neutral environment (pH = 7.4).

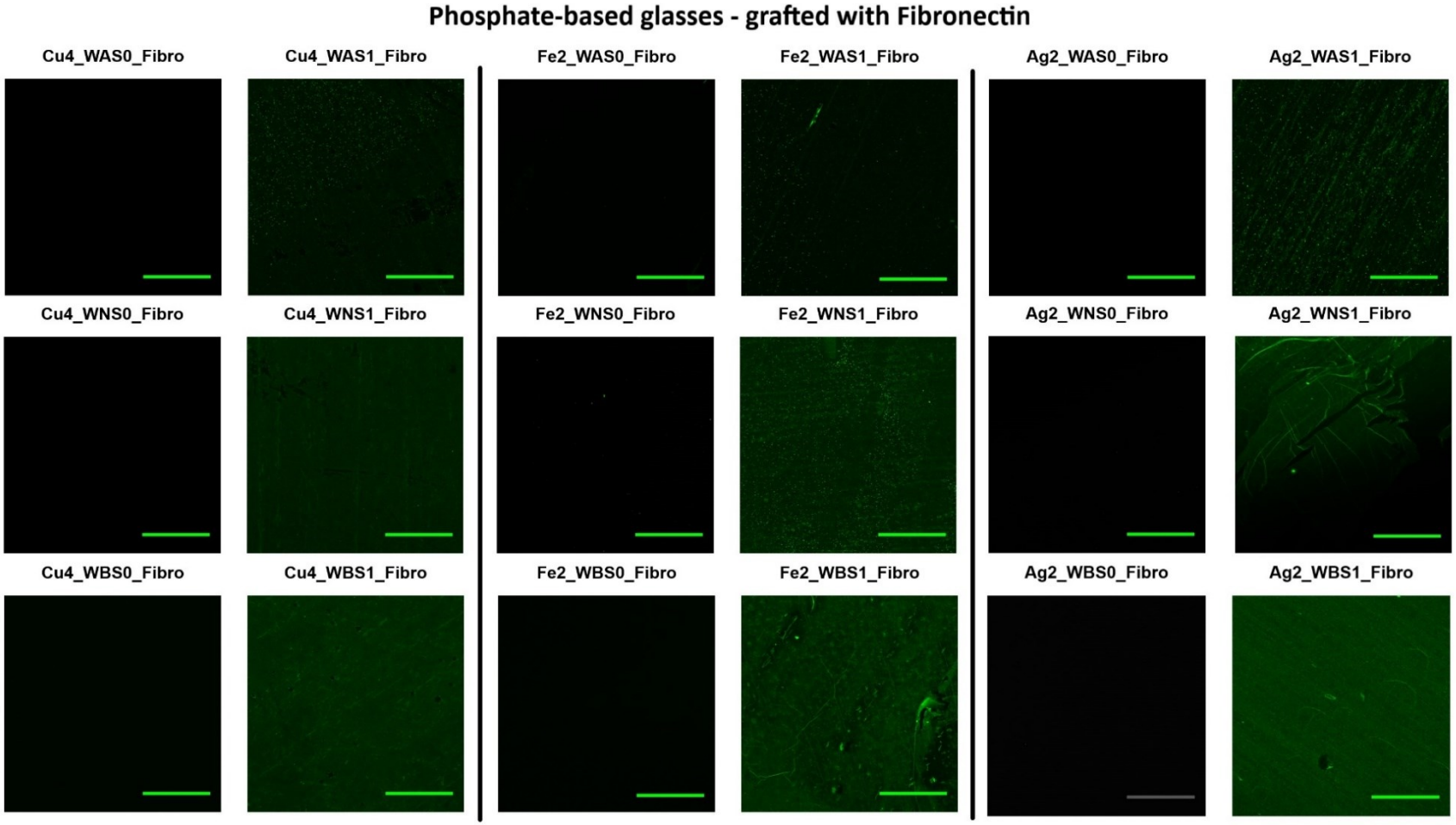

Figure 29. *Fluorescence images of Fibronectin-grafted phosphate-based glasses. Equipment: Nikon A1R+. Scale bar represents 100 µm.*

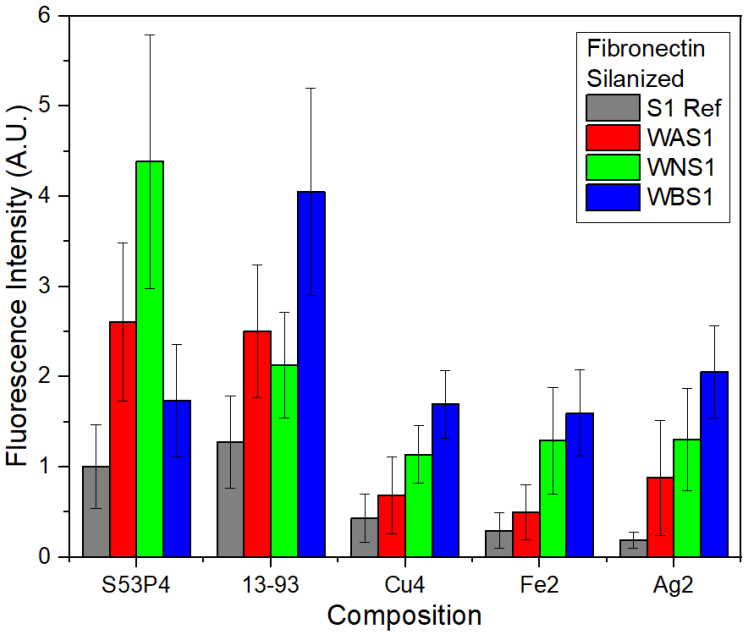

Figure 30. *Fluorescence intensity graph of fibronectin-grafted samples with APTES coating, extracted using ImageJ software.*

Phosphate-based glasses (figure 29) again exhibit much lower overall intensities than silica-based glasses. The remarkable increase in fluorescence intensity observed in all samples post silanization treatment further confirms the effects of APTES in improving the poor inherent protein adsorption of phosphate-based bioactive glasses. Meanwhile, the gradual and consistent increase of signals with increasing pH value of fibronectin solutions in these samples as well as in silica-based ones leads to the conclusion that basic environment (pH = 9.0) is the preferential condition for grafting fibronectin. The fluorescence intensity graph in figure 30 also shows a dominance in intensity associated with samples that were grafted with fibronectin in basic environment, which agrees with the visual evaluation.

The fluorescence images of fibronectin grafted samples not only once again confirm the effectiveness of silanization treatment in supporting the adsorption of both types of proteins but also show a more straightforward result where basic environment is considered the favorable environment for fibronectin grafting.

The contrast in the preferential environment of the two proteins could be explained by their different “tastes” towards hydrophobic/hydrophilic surfaces. Not only known for their abundance in the plasma, serum albumin has also been found to exhibit high affinity toward hydrophilic surfaces with strong binding strength (Jeyachandran et al. 2009). According to FTIR results, acidic treated silica-based samples underwent rapid dissolution with sign of HCA formation and surface hydration, rendering them to be more hydrophilic, thus more capable in immobilizing BSA than samples washed with solutions of other pH values. Meanwhile, FTIR spectra of basic washed samples showed almost no surface hydration, meaning that they might appear more hydrophobic post basic washing.

The high intensities recorded in these surfaces when grafted with fibronectin agrees with Grinnell and Feld' study in 1981 where hydrophobic surfaces were found to have more fibronectin present than hydrophilic ones although the adsorbed fibronectin on the later retained better bioactivities than those on the former.

Although information on conformational changes on adsorbed proteins is desirable, it is difficult to obtain. Many studies used special FTIR methods and meticulously analyzed the amide I and II bands from 1600 – 1750 cm^{-1} to determine the ratio of alpha helix, beta pleated sheet and beta turn to evaluate this aspect (Magyari et al. 2012, Gruian et al. 2012, Buchanan & El-Ghannam 2009). However, the FTIR spectra of protein-grafted samples obtained in both ATR and transmission modes were distorted and failed to reveal any specific trace of amide I and II bands which are also easily mistaken with O–H bending mode on hydrated samples, thus hindering the investigation on this aspect. In another study by Kim & Somorjai (2003), the combination of Infrared-visible sum frequency generation (SFG) vibrational spectroscopy fluorescence microscopy was employed to reveal the degree of protein spreading by investigating the tilting angle of methyl (CH_3) groups. The results were combined with previous studies using circular dichroism (CD) and X-ray reflectivity to obtain the information about the denaturation extent of various protein species when varying the bulk concentration of the protein solutions (Kim & Somorjai 2003). In a study back in 1981, Grinnell and Feld indirectly predicted the conformations of adsorbed fibronectin by treating them with antibodies or with radio-labeled fibronectin and evaluating the reactivity between them. Again, the lack of equipment and the solid monolithic form of the samples forced us to abandon this attempt.

4.3 Cell tests

Wild-type Mouse Embryonic Fibroblasts (MEFs) were cultured on bioactive glass samples to correlate the effects of surface treatments with and without fibronectin on the cell adhesion capacity. As concluded in the previous part, fibronectin adsorption was favoured on samples washed in basic buffer solution and functionalized with APTES. The three conditions chosen for these cell culture experiments, therefore, were untreated (negative reference), basic washing and silanization (WBS1) and the same condition plus coating with fibronectin prior to cell plating (WBS1+Fn).

The outcome of EVOS live imaging session was a series of images taken at predetermined beacons which could be used to create a time lapse video of a small portion of cell populations. A rating system was established to evaluate and give the overview on the prospect of cell adhesion and proliferation in different conditions. In this rating system, (-) mark indicates cell death and when there were cells alive, a number out of 5 stars (*) was given to that condition depending on the thriving prospect of the considered cell population.

Table 6. *An example of rating system in one cell culturing experiment.*

	Untreated	**WBS1**	**WBS1_Fn**	**Reference**
S53P4	Poor adhesion * 	Nice adhesion High density *****	Fairly good Low density ***	Normal Glass Coverslip_Fn ****
Ag2	Cell death -	Nice adhesion High density ***	Cell death -	Normal Glass Coverslip ***
Sr50	Poor adhesion *	Excellent adhesion *****	Excellent adhesion ****	Empty well

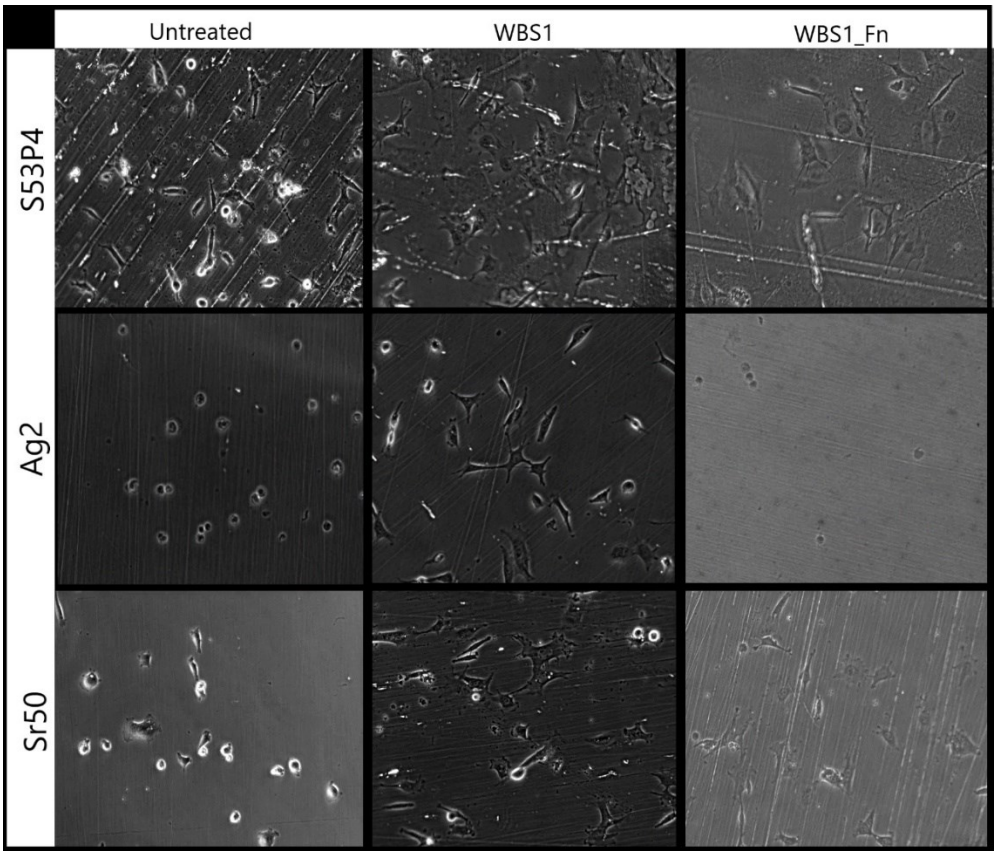

Figure 31. *A set of images extracted from the EVOS live imaging - taken at the same timepoint – on various glasses – recording the cell adhesion and proliferation as a function of surface modification.*

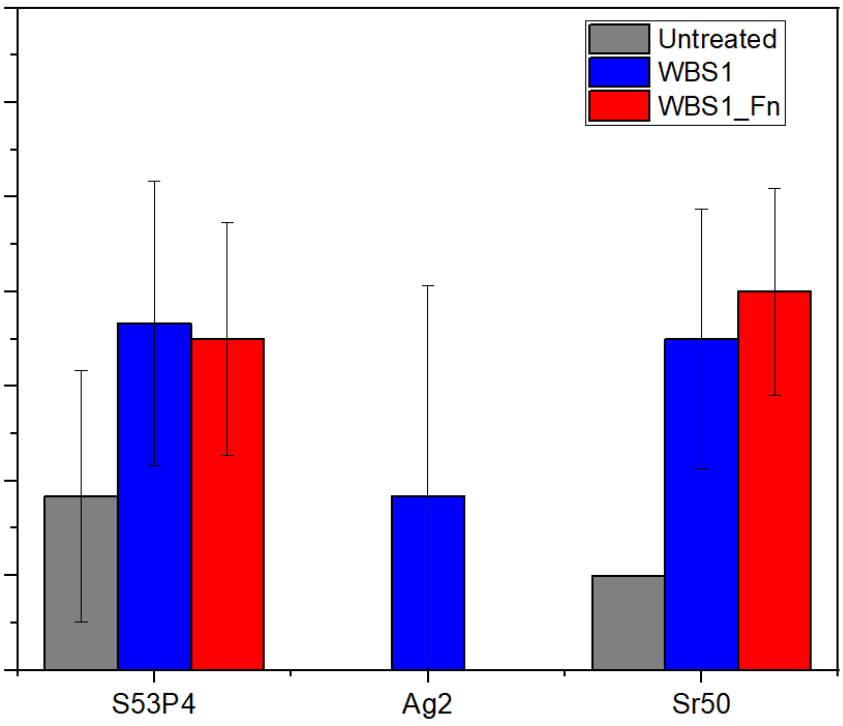

Figure 32. *Average rates of cell adhesion on different conditions.*

The outcomes of these cell culturing tests were also converted into numeric data, e.g. 0, 1, 2, 3, 4, 5 with (-) mark equals 0, and compared to get an overview of the EVOS® imaging outcome, one example of which is presented in figure 31. From the graph of average values and standard deviation of the rating (Figure 32), the surface treatments, i.e. washing in basic buffer solution, APTES coating and fibronectin grafting, show an improvement in cell adhesion on S53P4 and Sr50 bioactive glasses.

As seen from figure 31, treatment of the glass surface using a basic buffer solution and successively grafting silane at the glass surface led to a significant improvement in early cell attachment on all glass studied. The improved cell attachment was more pronounced at the surface in the two phosphate glasses, i.e. Sr50 and Ag2. Further protein grafting did not seem to further improve the early cell attachment on S53P4 and Sr50 glasses. Surprisingly, the cells did not attach on the fibronectin coated Ag2 samples. Further studies are ongoing in the group to better understand the surface modification occurring at the glass surface to explain such behavior. One possibility would be that during the cell culture, a significant amount of silver ions might have been released, resulting in a negative impact on cell adhesion and proliferation. Another possibility is that the extended surface treatment leads to a phosphate surface thereby the phosphate content is greater and therefore the glass dissolution is increase. It is known that glasses with high phosphate content do not promote cell attachment (Massera et al. 2015).

Another eventuallity is that, the APTES layer might wear off overtime leading to surface similar to the untreated one. The samples, prior to cell test were all and the silver ion

leaching rate might increase depending on the environment, leading to either an early cell death as seen in the fibronectin grafted samples (Ag2_WBS1_Fn) which has been immersed in aqueous PBS for 2 hours prior to cell plating or a prolonged barrier effect when soaking in cell culture medium (Ag2_WBS1).

Due to the rough surface of bioactive glass samples and the low resolution and low contrast of the brightfield images, it is difficult to give more than a rough overview of the cell populations or the effects of fibronectin grafting by the visual evaluation. Therefore, staining cells and fluorescence imaging were conducted to eliminate the background and highlight different aspects of the cell populations such as cell geometry, size, spreading manners and amount of focal adhesions detected.

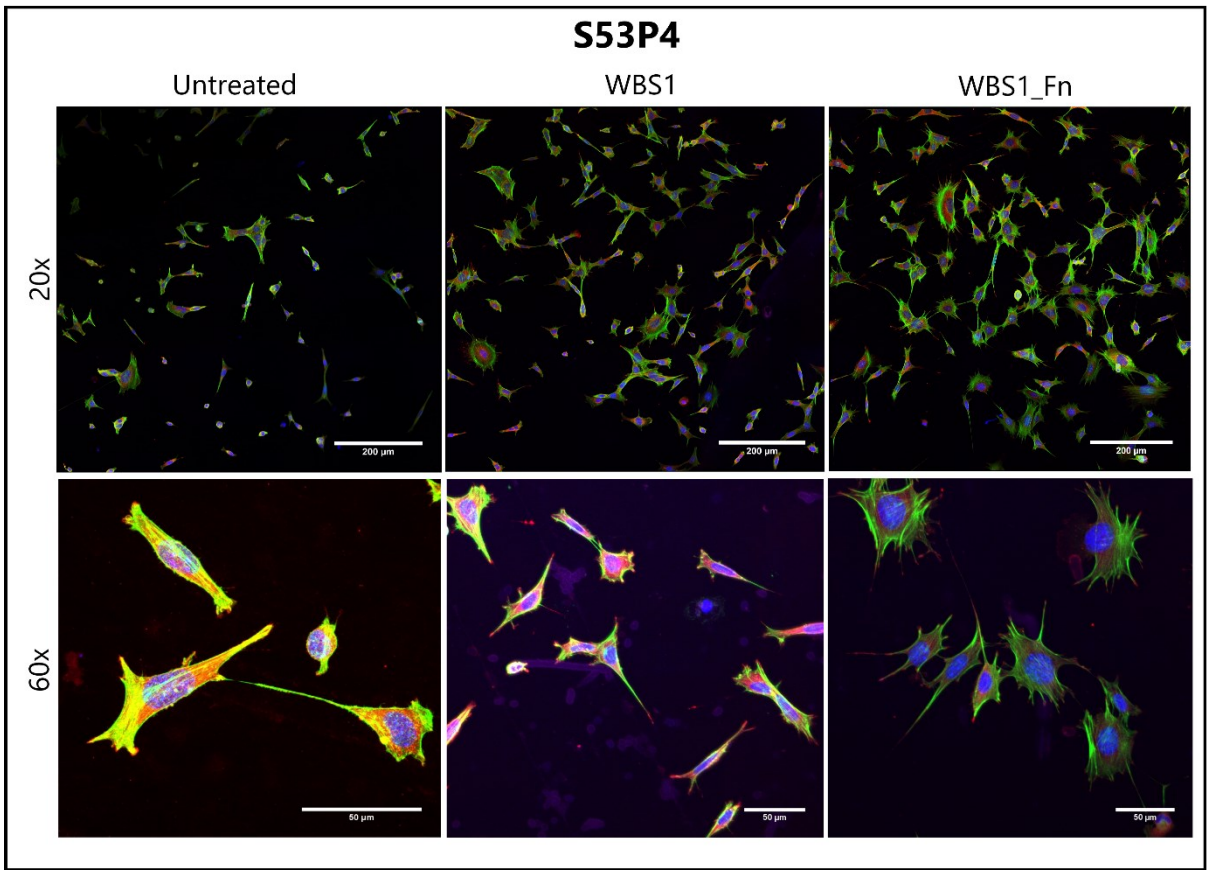

Figure 33. *Fluorescence images of cell populations cultured on S53P4 samples (silica-based). The above and below images were taken with 20x and 60x magnifying power, respectively.*

Fluorescence images of the cell populations cultured on S53P4 in 3 different conditions as presented in figure 33, show a notable improvement in cell adhesions and growth in samples with surface treatments and fibronectin coating. Mouse embryonic fibroblasts (MEFs) cultured on untreated S53P4 sample remained small and contracted on the glass surface. A large number of the cells on this sample were round, thick and small with little cytoskeleton (green actin filaments) detected and diameter mostly less than 20 µm. This

cellular configuration suggests that fibroblasts had difficulties finding suitable anchoring points and spreading on untreated samples.

The situation was improved in samples that were washed and functionalized with APTES. Cells grew larger and spread more widely on treated surface than on untreated surface. Diameter of cells on this sample are typically ranging from 20-30 µm for spreading cells. Even those elongated cells had bigger nuclei and stretched longer than their counterparts in untreated samples. Cytoskeletons were also well-highlighted with several actin filaments in green.

However, the most thriving cell population was observed in samples with fibronectin coating. Here the fibronectin grafting seems to have allowed fibroblasts to anchor tightly to the surface with a large number of focal adhesions detected in multiple directions instead of limited at longitudinal directions as in the untreated samples and those without fibronectin. A majority of the cell populations stretched flat and reach to a diameter ranging from 40 – 50 µm, suggesting fibroblasts were able to make multiple strong and stable focal adhesions with the surface.

The cell fixing and staining processes on Sr50 glass (phosphate-based), as presented in figure 34, was not as favourable as on S53P4 glass. Cell populations cultured on this glass were significantly washed off and affected during these processes, which was possibly due to the fast dissolution of this composition when coming in contact with aqueous PBS. Such behavior was already found in previous research from the group but are not yet published. Because of this unfortunate issue, the fluorescence images of this composition might only reflect cellular configuration but not the true distribution of cells on the glass surface and only the images of treated surfaces (WBS1 and WBS1_Fn) were captured. Cell staining was not performed on samples of the other phosphate-based composition – Ag2 due to cell death. Due to the complication of fast surface dissolution of these phosphate-based glasses, cell staining on these substrates should be conducted with great care and optimized if possible, e.g. by reducing PBS washing duration and frequency, to minimize the loss and damage to cell populations in future endeavours.

However, despite the damages to the cell population, a similar improvement of cell adhesion and spreading by the fibronectin grafting was observed in this image set of Sr50 samples. While most of the cells on the surface without fibronectin coating were thin (crosswise width from 5 – 15 µm) and stretching with a few focal adhesions detected in longitudinal directions, fibroblasts on fibronectin coated surface expanded widely (around 20 - 40 µm) with multiple focal adhesions detected also in directions other than longitudinal ones.

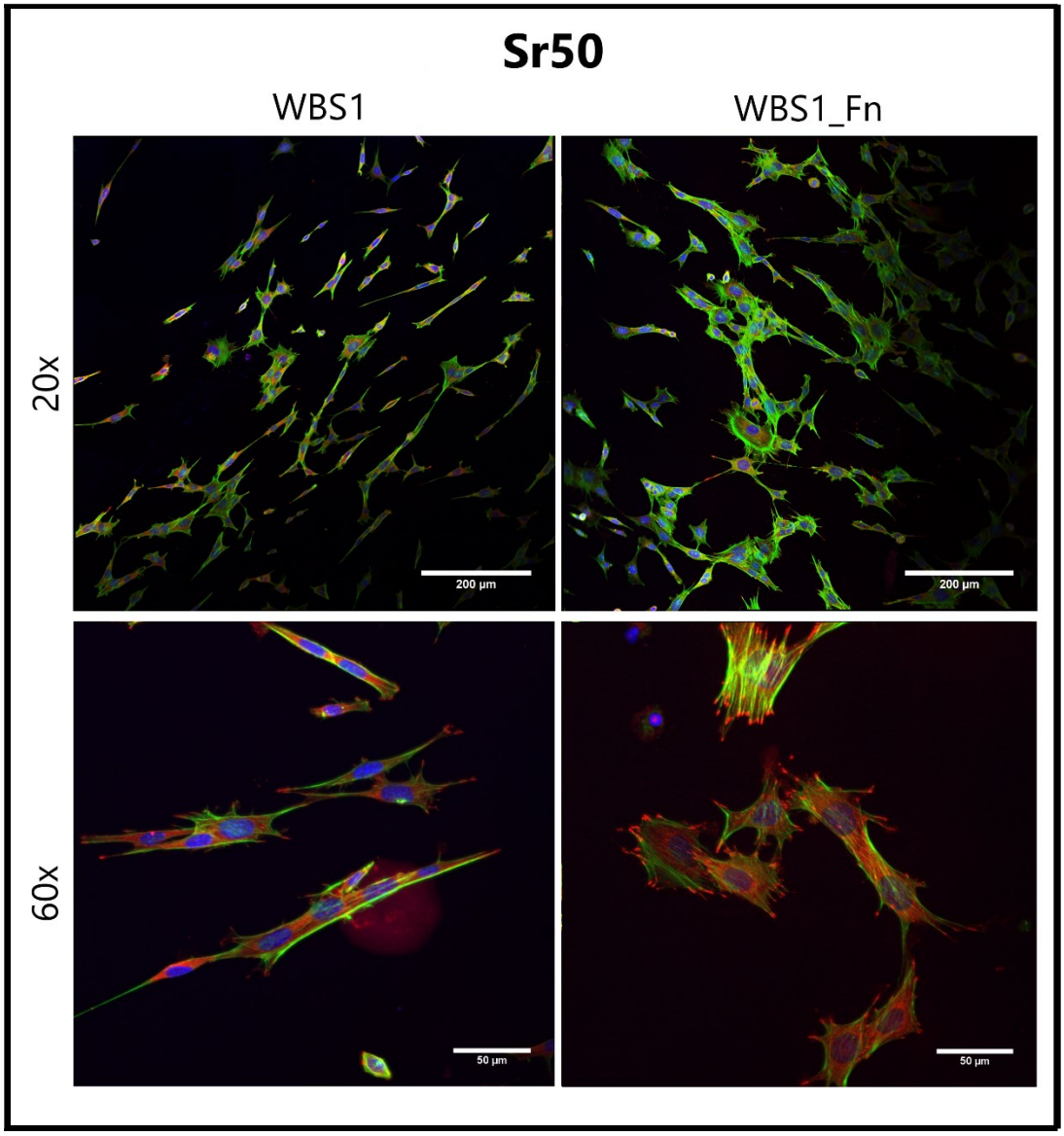

Figure 34. *Fluorescence images of cell populations cultured on Sr50 samples (phosphate-based glass). The above and below images were taken with 20x and 60x magnifying power, respectively.*

Considering all above aspects of the cell culture studies using MEFs, one can unambiguously say that while the silicate surface is favourable to cell attachment and proliferation, a surface treatment with a basic buffer solution enables to improve the cell interaction with the glass surface. Further adsorption of fibronectin at the glass surface was found to favour even more cell attachment and spreading at the glass surface by providing higher density of anchorage point for the studied cells.

The studied phosphate glasses were known from previous study for their poor capacity in supporting cell attachment. However, we know that the phosphate glass dissolution by-products are beneficial to the cell activity. Indeed, it was found that the cells grew well at the surrounding of the glass surface. Upon silanization of the glass surface, the cell attachment was greatly improved. As already seen in the case of silicate, the grafting of

fibronectin did further improve the cell attachment and spreading of the cells at the undoped-phosphate glass surface. Although the protein fluorescence images showed that less fibronectin was present on the surface of phosphate glasses than silicate glasses, which can be attributed to the lower concentration of silane being grafted at the surface of phosphate glasses, compared to the silicate, the cell attachment and spreading on these surfaces is considered competent, perhaps only a bit inferior to that of the silicate counterparts. However, a better protocol needs to be developed to preserve the true cellular configuration and distribution and ultimately to provide a better basic for a meaningful comparison.

Finally, the surface treatment of Ag2 phosphate glasses requires further investigation. The Ag doped phosphate glasses are known to be more reactive than the undoped glass. Thus, this could lead to degradation of the silane/protein layer during the pre-incubation and during cell culture. This in turn leads to poor attachment of cells when the surface was first washed and silanized and successively protein grafted. Eventually, the release of Ag should be quantified to assess if the Ag concentration in the culture medium reaches toxic concentrations.

5. CONLUSIONS

This study investigated the aspect of protein adhesion of 5 bioactive glass compositions and possible influential factors such as wettability, surface chemistry and pH values of protein solutions using 2 model proteins: bovine serum albumin (BSA) and fibronectin. Surface treatments including washing in buffer solutions of varied pH values and functionalization with (3-aminopropyl)triethoxysilane (APTES) were performed to improve their intrinsic affinity to these 2 proteins. The effects of these surface treatments were investigated by contact angle measurements and FTIR. The results showed that the preliminary washing did improved the wettability of phosphate-based glass surfaces and while APTES grafting increased contact angle, it enhanced the protein adhesion by the introduction of compatible functional groups with protein chemical structure. The varied pH values also brought some changes in the chemical structure, which are rapid dissolution, formation of HCA and surface hydration with low pH value, to silica-based glasses (S53P4 and 13-93) based on ATR-FTIR spectra.

Fluorescence imaging of protein grafted surfaces showed a significant increase of protein density as well as a more uniform protein layer on surfaces coated with APTES for both BSA and fibronectin. In additions, BSA displayed a preference for acidic grafting environment while fibronectin's most favourable grafting condition was in basic buffer solution, which could be attributed to their affiliation to hydrophilic and hydrophobic surfaces, respectively. This improved fibronectin adhesion on bioactive glasses brought by the surface treatments was later proved to provide a better support towards fibroblast adhesion and growth by live imaging and fluorescence imaging of immunohistochemically stained fibroblasts. Fibroblasts cultured on fibronectin grafted surface spread more widely and featured more focal adhesions in multiple directions compared to surface without the fibronectin.

The improvement in cell adhesions and spreading was seen in both silicate and phosphate glasses in a comparable degree, leading to the conclusion that these surface treatments, namely washing and grafting APTES on the surface as well as using basic environment as fibronectin grafting environment, therefore, seems to be an effective pathway to raise the compatibility of these novel compositions to proteins and cells. The knowledge of preferential grafting conditions for BSA and fibronectin could be used to design a preliminary treatment to achieve a required level of cell adhesion for certain biomedical applications.

Besides these exciting findings, this thesis work also brought up a few unsolved problems. The first problem is the stability APTES coating layer on the bioactive glasses. The second problem is that conformational changes of the adsorbed proteins have not been successfully investigated due to the lack of equipment and precedent protocols. Lastly, the

largely damaged cell populations during immunohistochemical staining processes poses the needs to optimize the protocols for this specific class of materials. Further investigations on these problems would provide an in-depth understanding on the APTES effectiveness in capturing proteins on bioactive glasses for long term as well as the true configuration of protein layers.

REFERENCES

Anderson, J. M, Rodriguez, A. and Chang, D. T. (2008). Foreign body reaction to biomaterials, *Seminars in Immunology*, vol. 20, (2), pp. 86-100. Available at: https://doi.org/10.1016/j.smim.2007.11.004.

Badylak, S., Gilbert, T. and Myers-Irvin, J. (2008). The Extracellular Matrix as a Biologic Scaffold for Tissue Engineering. In C. A. v. Blitterswijk, ed., Tissue Engineering, Boston: Academic Press, pp. 121-143.

Barrère, F., Ni, M., Habibovic, P., Ducheyne, P. and Groot, K.d. (2008). Degradation of bioceramics. In C. A. v. Blitterswijk, ed., Tissue Engineering, Boston: Academic Press, pp. 223-254.

Bourhis, E. L. (2014). Glass: Mechanics and Technology. 2nd ed. Weinheim: John Wiley & Sons, Inc., pp. 55-84.

Brentrup, G. J., Moawad, H. M., Santos, L. F., Almeida, R. M. and Jain, H. (2009). Structure of $Na_2O–CaO–P_2O_5–SiO_2$ Glass–Ceramics with Multimodal Porosity, Journal of the American Ceramic Society, Vol. 92, (1), pp. 249-252.

Buchanan, L.A. and El-Ghannam, A. (2009). Effect of bioactive glass crystallization on the conformation and bioactivity of adsorbed proteins, Journal of Biomedical Materials Research - Part A, vol. 93, no. 2, pp. 537-546.

Cao, W. & Hench, L.L. (1996). "Bioactive materials", Ceramics International, vol. 22, no. 6, pp. 493-507.

Chang, J., Zhou, Y.L. & Zhou, Y. (2011). Surface modification of bioactive glasses. In H. Ylänen, ed., Bioactive Glasses: Materials, Properties and Applications, Woodhead Publishing, pp. 29-52.

Dee, K.C., Puleo, D.A. & Bizios, R. (2002). An Introduction to Tissue-Biomaterial Interactions. New York: John Wiley & Sons, Inc., pp. 1-52.

Fagerlund, S. and Hupa, L. (2017). Melt-derived Bioactive Silicate Glasses. In A. R. Boccaccini, D. S. Brauer and L. Hupa, ed., Bioactive Glasses: Fundamentals, Technology and Applications, Royal Society of Chemistry, pp. 1-26.

Ferraris, S. and Verné, E. (2017). Surface functionalization of bioactive glasses. In A. R. Boccaccini, D. S. Brauer and L. Hupa, ed., Bioactive Glasses: Fundamentals, Technology and Applications, Royal Society of Chemistry, pp. 220-229.

Jeyachandran, Y.L., Mielczarski, E., Rai, B. & Mielczarski, J.A. (2009). Quantitative and qualitative evaluation of adsorption/desorption of bovine serum albumin on hydrophilic and hydrophobic surfaces, Langmuir : the ACS journal of surfaces and colloids, vol. 25, no. 19, pp. 11614.

Johnson, M. B. and White, M. A. (2013). Thermal Methods. In D. W. Bruce, D. O'Hare, and R. I. Walton, ed., Multi Length-Scale Characterisation: Inorganic Materials Series, John Wiley & Sons, Inc., p. 64.

Jones, J. and Clare, A. (2012). Bio-Glasses: An Introduction. New York: John Wiley & Sons, Inc., pp. 66.

Gunawidjaja, P.N., Mathew, R., Andy Y. H. Lo, Izquierdo-Barba, I., García, A., Arcos, D., Vallet-Regí, M., Edén, M. (2012). Local structures of mesoporous bioactive glasses and their surface alterations in vitro: inferences from solid-state nuclear magnetic resonance. Philosophical Transactions: Mathematical, Physical and Engineering Sciences, vol. 370, pp. 1376-1399.

Grinnell, F. & Feld, M. K. (1982). Fibronectin adsorption on hydrophilic and hydrophobic surfaces detected by antibody binding and analyzed during cell adhesion in serum-containing medium, Journal of Biological Chemistry, Vol. 257. No. 9, pp. 4888-4893.

Gruian, C., Vanea, E., Simon, S. & Simon, V. (2012). FTIR and XPS studies of protein adsorption onto functionalized bioactive glass, BBA - Proteins and Proteomics, vol. 1824, no. 7, pp. 873-881.

Hench, L.L. (2006). The story of Bioglass, Journal of Materials Science: Materials in Medicine, vol. 17, no. 11, pp. 967-978.

Hupa, L. (2011). Melt-derived bioactive glasses. In H. Ylänen, ed., Bioactive Glasses: Materials, Properties and Applications, Woodhead Publishing, pp. 3-28.

Kim, J. and Somorjai, G. A. (2003). Molecular packing of lysozyme, fibrinogen, and bovine serum albumin on hydrophilic and hydrophobic surfaces studied by infrared-visible sum frequency generation and fluorescence microscopy, Journal of the American Chemical Society, vol. 125, (10), pp. 3150-3158.

Lamba, N.M.K., Baumgartner, J.A. & Cooper, S.L. (1998). Cell-synthetic surface interactions. In C. W. Patrick Jr. and and L. V. McIntire, ed., Frontier in Tissue Engineering, Oxford: Pergamon, pp. 121-137.

Leppäranta, O., Vaahtio, M., Peltola, T., Zhang, D., Hupa, L., Hupa, M., Ylänen, H., Salonen, J.I., Viljanen, M.K. & Eerola, E. (2008). Antibacterial effect of bioactive glasses on clinically important anaerobic bacteria in vitro, Journal of Materials Science: Materials in Medicine, vol. 19, no. 2, pp. 547-551.

Li, J., Chen, Y., Yin, Y., Yao, F. and Yao, K. (2007). Modulation of nano-hydroxyapatite size via formation on chitosan–gelatin network film in situ, Biomaterials, vol. 28, (5), pp. 781-790. Available at: https://doi.org/10.1016/j.biomaterials.2006.09.042

Lindfors, N. C., Koski, I. , Heikkilä, J. T., Mattila, K. and Aho, A. J. (2010a). A prospective randomized 14-year follow-up study of bioactive glass and autogenous bone as bone graft substitutes in benign bone tumors, Journal of Biomedical Materials Research, Vol. 94B, (1): pp. 157-164. Available at: https://doi.org/10.1002/jbm.b.31636

Lindfors, N.C., Hyvönen, P., Nyyssönen, M., Kirjavainen, M., Kankare, J., Gullichsen, E. & Salo, J. (2010b). Bioactive glass S53P4 as bone graft substitute in treatment of osteomyelitis, Bone, vol. 47, no. 2, pp. 212-218.

Magyari, K., Baia, L., Popescu, O., Simon, V. & Simon, S. (2012). The anchoring of fibrinogen to a bioactive glass investigated by FT-IR spectroscopy, Vibrational Spectroscopy, vol. 62, pp. 172-179.

Magyari, K., Baia, L., Vulpoi, A., Simon, S., Popescu, O., Simon, V. (2015). Bioactivity evolution of the surface functionalized bioactive glasses. Journal of Biomedical Materials Research Part B, Vol. 103B, (2), pp. 261–272. Available at: https://doi.org/10.1002/jbm.b.33203

Massera, J., Hupa, M. & Hupa, L. (2012). Influence of the partial substitution of CaO with MgO on the thermal properties and in vitro reactivity of the bioactive glass S53P4, Journal of Non-Crystalline Solids, vol. 358, no. 18-19, pp. 2701-2707.

Massera, J., Petit, L., Cardinal, T., Videau, J.J., Hupa, M. and Hupa, L. (2013). Thermal properties and surface reactivity in simulated body fluid of new strontium ion-containing phosphate glasses, Journal of Materials Science: Materials in Medicine, vol. 24, no. 6, pp. 1407-1416.

Massera, J., Kokkari, A., Närhi, T. & Hupa, L. (2015). The influence of SrO and CaO in silicate and phosphate bioactive glasses on human gingival fibroblasts, Journal of Materials Science: Materials in Medicine, vol. 26, no. 6, pp. 1-9.

Massera, J., Mishra, A., Guastella, S., Ferraris, S. and Verné, E. (2016). Surface functionalization of phosphate-based bioactive glasses with 3-aminopropyltriethoxysilane (APTS), Biomedical glasses, vol. 2, no. 1.

Mishra, A., Rocherullé, J. & Massera, J. (2016). Ag-doped phosphate bioactive glasses: thermal, structural and in-vitro dissolution properties, Biomedical Glasses, vol. 2, (1), pp. 38-48.

Mishra, A., Petit, L., Pihl, M., Andersson, M., Salminen, T., Rocherullé, J., Massera, J., (2017). Thermal, structural and in vitro dissolution of antimicrobial copper-doped and

slow resorbable iron-doped phosphate glasses, Journal of Materials Science, vol. 52, no. 15, pp. 8957-8972.

McKenzie, J.L. and Webster, T.J. (2009). Protein interactions at material surfaces. In R. Narayan, ed., Biomedical Materials, Boston: Springer US, pp. 215-237.

McAndrew, J., Efrimescu, C., Sheehan, E. and Niall, D. (2013). Through the looking glass; bioactive glass S53P4 (BonAlive®) in the treatment of chronic osteomyelitis, Irish Journal of Medical Science, vol. 182, no. 3, pp. 509-511.

Rahaman, M.N., Day, D.E., Sonny Bal, B., Fu, Q., Jung, S.B., Bonewald, L.F. & Tomsia, A.P. (2011). Bioactive glass in tissue engineering, Acta Biomaterialia, vol. 7, no. 6, pp. 2355-2373.

Saiz, E., Goldman, M., Gomez-Vega, J.M., Tomsia, A.P., Marshall, S.J. & Marshall, G.W. (2002). In vitro behavior of silicate glass coatings on Ti6Al4V, Biomaterials, vol. 23, no. 17, pp. 3749-3756.

Scheibe, HJ., Drescher, D., Kolitsch, A. and Mensch, A. (1995). Investigation of surface topography, morphology and structure of amorphous carbon films by AFM and TEM, Fresenius Journal of Analytical Chemistry, Vol. 353, (5-8), pp. 690-694. Available at: https://doi.org/10.1007/BF00321351

Serra, J., Serra, C., González, P., Liste, S., Chiussi, S., León, B., Pérez-Amor, M., Ylänen, H.O. and Hupa, M. (2003). FTIR and XPS studies of bioactive silica-based glasses, Journal of Non-Crystalline Solids, vol. 332, no. 1, pp. 20-27.

Stuart, B. H. (2005). Inorganic Molecules. In D. J. Ando and B. H. Stuart, ed. Infrared Spectroscopy: Fundamentals and Applications, John Wiley & Sons, Ltd, pp. 95-111.

Williams, D. (2008). Biocompatibility. In C. A. v. Blitterswijk, ed., Tissue Engineering, Boston: Academic Press, pp. 255-278. Available at: https://doi.org/10.1016/B978-0-12-370869-4.00009-4

Wang, H., Cao, Y., Sun, Y., Wang, K., Cao, C., Yang, L., Zhang, Y., Zheng, Z., Li, D., Wang, J. & Han, Y. (2011). Is there an optimal topographical surface in nanoscale affecting protein adsorption and cell behaviors?", Journal of Nanoparticle Research, vol. 13, no. 9, pp. 4201-4210.

Wang, K., Zhou, C., Hong, Y. and Zhang, X. (2012). A review of protein adsorption on bioceramics, Interface Focus, vol. 2, no. 3, pp. 259-277.

Ylänen, H. (ed.). (2011). Bioactive Glasses: Materials, Properties and Applications, Woodhead Publishing.

Zeitler, T.R. and Cormack, A.N. (2006). Interaction of water with bioactive glass surfaces", Journal of Crystal Growth, vol. 294, no. 1, pp. 96-102.

APPENDIX A: FULL FTIR SPECTRA OF PHOSPHATE GLASSES

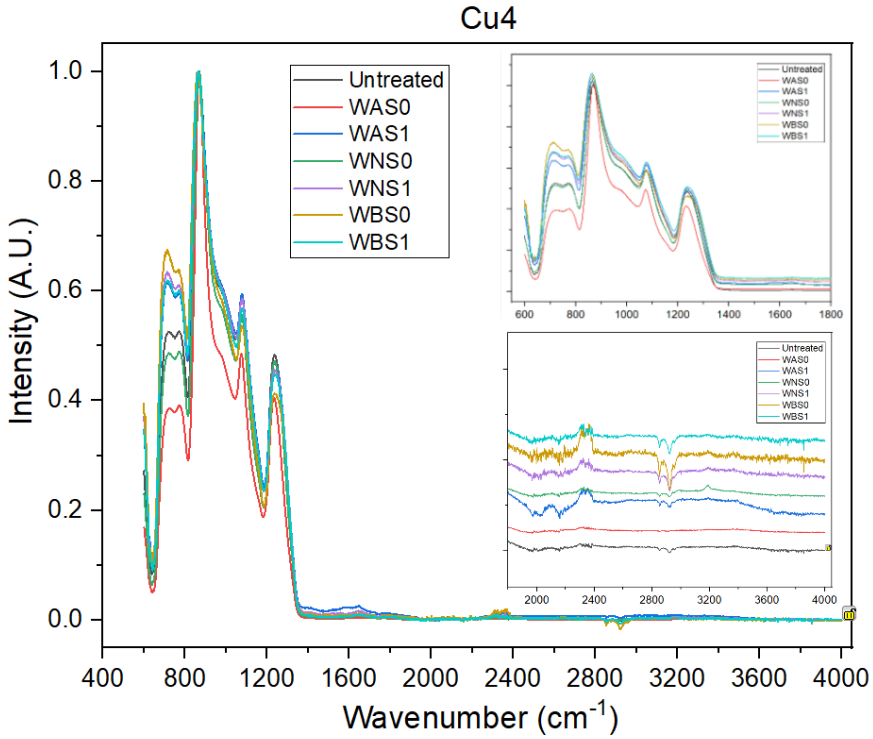

Figure A. *FTIR spectra of Cu4 phosphate glass.*

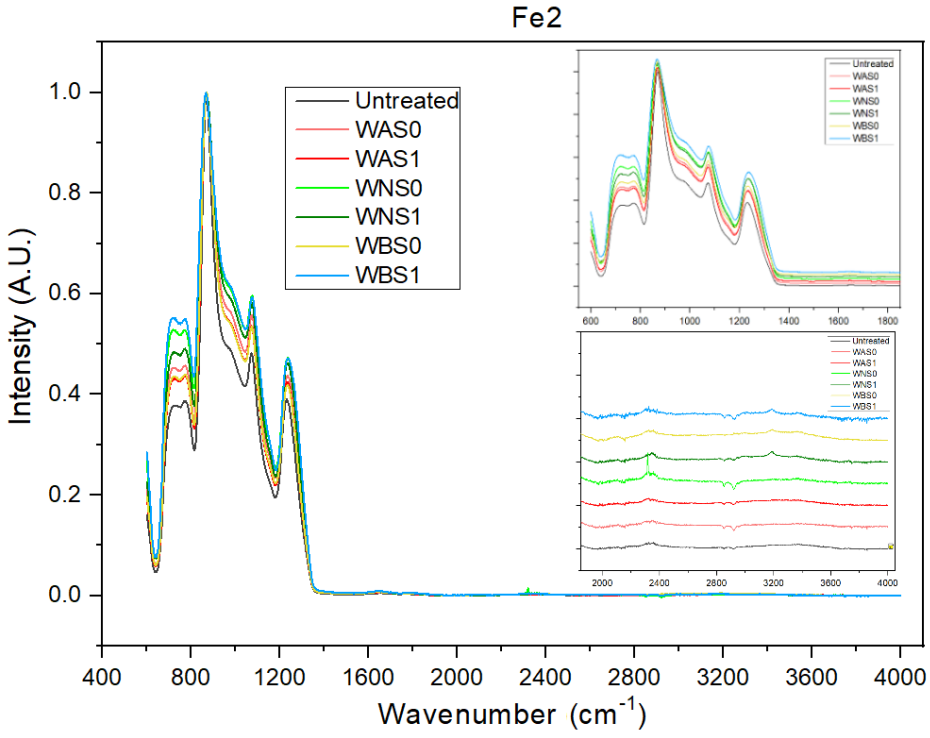

Figure B. *FTIR spectra of Fe2 phosphate glass.*

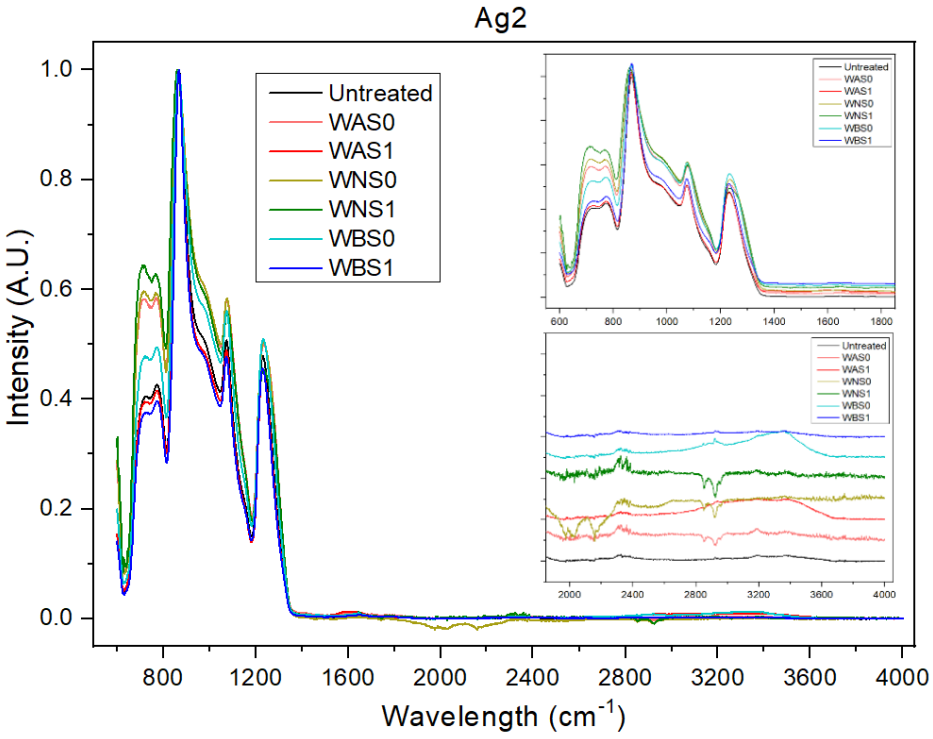

Figure C. *FTIR spectra of Ag2 phosphate glass.*